Recent Advances in Nature Inspired Solutions for Ground Engineering (NiSE)

Arya Assadi-Langroudi[1,*]; Brendan C. O'Kelly[2]; Daniel Barreto[3]; Federica Cotecchia[4]; Henry Dicks[5]; Abdullah Ekinci[6]; Fernando Estéfan T. Garcia[7]; Michael Harbottle[8]; Vito Tagarelli[4]; Ian Jefferson[9]; Pooneh Maghoul[10]; Enrico Masoero[11]; Gráinne El Mountassir[12]; Balasingham Muhunthan[13]; Xueyu Geng[14]; Soheil Ghadr[15]; Mehdi Mirzababaei[16]; Helen Mitrani[11]; Leon van Paassen[17]

[1,*] Department of Engineering and Construction, University of East London, England, E16 2RD, UK. ORCID https://orcid.org/0000-0003-3657-552X [Corresponding Author – A.AssadiLangroudi@uel.ac.uk]

[2] Department of Civil, Structural and Environmental Engineering, Trinity College Dublin, Dublin, D02 PN40, Ireland. ORCID https://orcid.org/0000-0002-1343-4428

[3] Edinburgh Napier University, Edinburgh, Scotland, UK

[4] Politecnico di Bari, Bari, Italy

[5] University of Leeds, Leeds, England, UK

[6] Middle East Technical University, Güzelyurt, Cyprus

[7] University of Michigan, Ann Arbor, USA

[8] Cardiff University, Cardiff, Wales, UK

[9] University of Birmingham, Birmingham, England, UK

[10] University of Manitoba, Winnipeg, Canada

[11] Newcastle University, Newcastle, England, UK

[12] University of Strathclyde, Glasgow, Scotland, UK

[13] Washington State University, Pullman, USA

[14] Warwick University, Coventry, England, UK

[15] National Cheng Kung University, Tainan, Taiwan

[16] Central Queensland University, Melbourne, Australia

[17] Arizona State University, Phoenix, USA

For potential publication in International Journal of Geosynthetics and Ground Engineering
https://www.springer.com/journal/40891 ; https://www.scopus.com/sourceid/21100913564#tabs=1

Abstract

The ground is a natural grand system; it is composed of myriad constituents that aggregate to form several geologic and biogenic systems. These systems operate independently and interplay harmoniously via important networked structures over multiple spatial and temporal scales. This paper presents arguments and derivations couched by the authors, to first give a better understanding of these intertwined networked structures, and then to give an insight of why and how these can be imitated to develop a new generation of nature-symbiotic ground engineering techniques. The paper draws on numerous recent advances made by the authors, and others, in imitating forms (e.g., synthetic fibres that imitate plant roots), materials (e.g., living composite materials, or living soil that imitate fungi and microbes), generative processes (e.g., managed decomposition of construction rubble to mimic weathering of aragonites to calcites), and functions (e.g., recreating the self-healing, self-producing, and self-forming capacity of natural systems). Advances are reported in three categories of Materials, Models, and Methods (3Ms). A novel value-based appraisal tool is also presented, providing a means to vet the effectiveness of 3Ms as standalone units or in combinations.

Keywords: Biomimicry; Soil; Improvement; Self-heal; Natural.

Declaration

Funding: This paper is made available through contributions of authors to the NiSE1 Workshop, which was helped through financial assistance of the National Research Foundation, Department of Science and Technology South Africa, and The Royal Society UK, through the Newton Fund DST-NRF NFPF170627245562 grant.

Conflicts of interest/Competing interests: None.

Availability of data and material: None.

Code availability: Not Applicable.

Ethics approval: Not Applicable.

Consent to participate: Co-authors agree to participate in publication of this paper.

Consent for publication: Co-authors agree to participate in publication of this paper.

Author's contribution statement: AAL ([1]) steered the discussions among the team and has written up the paper. BCO ([2]) edited the paper and co-steered discussions among the team. DB ([3]), FETG ([7]), AE ([6]), and MH ([8]) provided inputs on analytical methods. IJ ([9]) and AAL ([1]) developed the conceptual framework. HD ([5]) led, wrote and edited the philosophical backgrounds of NiSE. SG ([15]), MM ([16]) and XG ([14]) fed in, and contributed to, discussions on nature-inspired materials and laboratory-scale methods. FC ([4]) and VT ([4]) led the field-scale methods. LvP ([17]), HM ([11]), BM ([13]), GEM ([12]) led on, and fed into the bio-mediated methods. PM ([10]) contributed to multiple sections and offered a second round of editing. EM ([11]) led on meso-scale advanced models. All authors reviewed the paper and supported AAL ([1]) in getting the work to the presented state.

1. Introduction

1.1 Natural and Engineered Ground: Circularity and Man-made Disruptions

The ground is a grand system of systems. For provision of continual services, it deploys *mechanisms* that allow the constituting systems to interplay. Each system is made up of elements that are naturally adaptable, responsive, and constantly evolving. Systems have fractal properties at many levels. This means the characteristics of each system can be manifested in, or be predicted from, the properties of elements. Systems are self-healing, self-producing, and self-forming. This means elements in systems constantly evolve, adopt form and roles in response to environment, and re-establish functions that are disrupted in the natural erosive and stress environment. Collectively, these *constitutive properties* mark the fundamental difference between natural and engineered ground, as two different types of grand systems.

To better understand this difference, the critical transport infrastructure, taking London Underground (LU) as an example, may be considered as one type of an engineered grand system. The LU railway lines constitute of 300 m blocks, within which traffic is restricted to one train at any given time. The blocks are kept clear for passing trains through a 'signalling' technology. Trains stop running when signals fail. This can happen due to a short circuit in a wet day (causing disruption in how systems interact or *mechanisms*), but also occurs due to failure of any small component of the track (failure of systems or their components). In this respect, failure in any one system – in conventional engineered grand systems – will probably have cascading ramifications. On the other side of spectrum, take dune sand as an example of a natural grand system. Overall, dune sand can be inherently breakable. In the natural stress environment, groups of certain sized particles split to finer size. The breakage output appears in two forms, that is either aggregates of 'closely interlocked' and 'welded' fines, or a 'sea' of detached fines. Among the fines are mature particles that survive further breakage, and defected particles that break further into finer fragments. Both mature and defected particles adopt certain signature shapes. Among the aggregates are clast-like units that only break under large or anisotropic loads, or a prolonged course of stressing and through the mechanism of fatigue fracturing. Looser aggregates break into fines, some independent, and some in form of smaller sized aggregates. In this, the sorting, grading and mode-size distribution of sand are varied qualities. The structure is self-producing and self-healing, certain pronounced mode sizes continuously disappearing and reappearing. The components constantly evolve – in size and shape. During their lifetimes, components play various roles (e.g., as welding agents in clast-like aggregates that trap, compress and split fines into finer fragments, or as individual fines breaking into finer fractions), in response to environmental actions. Components have a capacity of re-establishing functions that are disrupted, and their constant evolution have fractal characteristics [1-2]. Owing to these varied and fractal features, failure of components (e.g., breakage of particles) would not disrupt the overall behaviour of the grand system.

Traditional (or conventional) engineered ground in the built environment context is a product of mechanical or chemical densification, with an often predominant mission of enhancing stiffness, and stress at steady states, at the cost of filling and compacting void spaces, and replacing air, water and microorganisms with calcium-based cements and alike. This transforms the natural ground into a self-standing (e.g., for cuttings), impermeable (to line buried wastes or control groundwater), strong and stiff (to bear superstructure loads) medium. However, this causes disruption to the biogeochemical cycles and self-forming, self-healing capacities of structures which are reliant on soils' intertwining pore network and driven by interaction amongst frame and bonding elements, and also the living organisms present.

1.2 Biomimicry: A Philosophical Perspective

At a general theoretical level, biomimetic or bio-inspired innovation involves observing natural systems, abstracting traits from those systems, and transferring those abstracted traits into engineering or design solutions [3]. While there exist numerous typologies covering the different basic types of traits that may be abstracted from nature [4-5], the ideal typology would be economical, such that there are as few basic traits as possible, comprehensive, such that all the basic traits are included, and coherent, such that the different traits fit together without overlapping, like the pieces of a jigsaw. Just such a typology may be established through drawing on Aristotle's doctrine of the four causes (see pp. 38-41 in [6]). From this perspective, there are only four basic types of traits we may abstract from nature and thereafter take as model: namely, forms, materials, generative processes, and functions.

In the case of the traits, we may abstract forms from the ground (understood as a natural system), such as rod-shaped, fibrous aragonite calcium carbonate in natural form, or as product of carbon sequestration in Ca–Mg silicates from construction and demolition wastes. As for the materials, they may be either abiotic (e.g., recycled and upcycled fibres, soils, etc.) or biotic (e.g., plants, micro-organisms, worms). Drawing on Aristotle, the concept of generative process covers both the generation of entities (producing) and the generation of effects (effecting) – see Ibid pp.39. In the case of the ground, examples of the former include bio-mineralization and humus formation, and examples of the latter include carbon sequestration and water infiltration. As for the functions, these are the roles the natural system plays in larger systems of which it is but a part. In the case of the ground, they may include such phenomena as habitat construction, climate regulation, erosion prevention, and soil stabilization. They differ from generative processes inasmuch as the same function may potentially be achieved using different processes; one may abstract from nature a specific function (e.g., soil stabilization) but realize it in quite different ways (e.g., mechanical as opposed to biological stabilization techniques).

The traits abstracted from nature may also be imitated at differing levels of abstraction. One may, for example, imitate the precise way that a specific species of plant stabilizes the soil. But one may also imitate the general principle – abstractable from any number of different natural ground systems – of stabilizing the soil using plant roots. As a general rule, the difference between biomimetics and bio-inspiration lies precisely in the fact that bio-inspiration works at higher levels of abstraction; it is general principles and techniques related to such desirable functions as soil stabilization, carbon sequestration, habitat provision, and so on, that are abstracted from nature, rather than concrete models derived from a specific natural system.

Lastly, it is also important to note that biomimetic and bio-inspired designs involve a further feature one may call "composition". If, as Aristotle maintains, both natural and design systems may be analysed in terms of forms, materials, generative processes, and functions, and if biomimetic or bio-inspired engineering involves abstracting these traits from natural systems and transferring them over to artificial systems, it is also true that one may abstract traits from different natural systems, and, in some cases at least, combine them with artificial traits devised by humans. An artificially engineered ground system may, for example, imitate both the forms and the functions of a natural ground system, while using artificial materials and while being generated using artificial processes. In such an instance, the artificial system would have been composed by joining together forms and functions abstracted from nature with materials and generative processes devised by humans. But, provided at least one trait has been imitated from nature for purposes of imitation, the artificial design may nevertheless be characterized as biomimetic or bio-inspired.

Drawing on this understanding of the process of biomimetic and bio-inspired innovation, the present contribution will present numerous advances in soil engineering that imitate – at varying levels of abstraction and in the context of varied compositions – at least one basic trait, whether form (e.g., synthetic virgin fibres that imitate plant roots in tying together loose soil particles), materials (e.g., living composite materials or living soil that imitate fungi and microbes), generative processes (e.g., managed decomposition of construction rubble inspired by geological transformation of aragonites to calcites – e.g., [7]), and functions (e.g., recreating the self-healing capacity of natural systems in the form of responsive materials).

1.3 Rethought Deliverables in Ground Engineering

Given the dual nature of engineered ground as, on the one hand, the cause of disordered ground ecosystem and, on the other, the stabilised bedding for earth structures and therefore the integral constituent of the built environment, it becomes a matter of urgency to ask whether there can be a generation of technologies, and by extension a rethought suite of materials, for preserving systems that underpin and service its natural functions. Ideally, engineering interventions need to transform the natural ground into a medium that continuously interplays with the environment around, adapts itself to changing weather, captures, conveys and retains precipitation waters, supports flora and fauna, stores and locks carbon, captures aerosols, eradicates dust efflux into air, absorbs contaminants and fixates buried domestic, rubble and demolition wastes and construction rubble to offer stability to subsurface and surface structures. The deliverables collectively shape a new way of thinking, '*primum non nocere'*, or *first do no harm* [then do some good]. Engineered ground should ideally retain its original fractal characteristics, double-porosity quality (in granular soils) and structure-dependent behaviour, self-healing capabilities and mineralisation in response to fatigue and entropy. This ideal engineered ground in illustrated in Figure 1a, in the context of NiSE, short for Nature-inspired Solutions for ground Engineering.

1.4 NiSE – the Framework

The NiSE deliverables are used to develop an adaptability indicator system and assessment method for evaluating different stabilising materials (and structures that evolve from the introduction of such materials to soil). Fig 1b presents a suite of indicators, or performance criteria, as well as a traffic-light scoring system that indicates the performance of materials based on the adaptation of the NiSE initiative. Indicators are deliberately without weightings to avoid subjectivity and to allow the model to be deployed globally and across multiple sectors and disciplines. Figure 1b is the blueprint of the NiSE initiative and provides a potential chance to be utilised as a value-based decision support framework for emerging ground engineering techniques. The five-point scoring scale is applied to each material in three primary categories of processes, forms and functions. The cumulative score for each material is a quantitative measure of a technique's impact within the NiSE context.

Fig. 1 (a) NiSE five principal aims and interlinked deliverables; (b) NiSE deliverables as indicators of materials' performance, measured by a traffic-light scoring system: the framework can be applied to candidate stabilising materials in any project

The principal objectives of this paper is to collate latest advances in materials, methods and models that underpin these novel ground engineering interventions, to discuss their development and deployment within the biomimetic or bio-inspired innovations context, and their common deliverables: (1) preserved permeability and porosity, (2) balanced water retention and conveyance capacity, (3) durability in the face of low-order cyclic, transient or extreme-but-one-off actions (thermo-hydro-chemo-mechanical), (4) enhanced strength, stiffness and particularly small-strain stiffness, (5) enhanced steady states (quasi-steady state, ultimate steady state, phase transformation, critical state) and relaxed flow potential, (6) enhanced resilience in the face of extreme events, (7) adaptability to wider loading environment: hydrodynamic, cyclic, and anisotropic.

2. Advances in Models and Methods

The overall vision – within the context of NiSE – is to explore prospects for developing and deploying models and methods that enable capturing the behaviour of the porous multimodal soil medium, and for developing mediated soil materials that are inspired by or imitate nature.

2.1 Soils and Particulate Matters Alike

Models and methods vary across the spectrum of scales.

For clays with a median sub-2μm particle size, the flat platy shape of particles, high ratio of surface area to volume, and surface charges influence clay behaviour. For soft clays, in particular, accurate understanding of complex soil behaviour is possible at nanoscale and is paramount to admissible serviceability of structures, slopes, and earthen transport-infrastructure embankments, to name a few. At the nanometre scale, rigorous solutions to the underlying physics are possible and can be fully predicted. In fact, innovation is created at nanoscale. Molecular dynamics (MD) simulation is an example of nanoscale techniques that are used to explore the interaction between colloidal clay nano-platelets, their orientation and inherent anisotropy. The impacts of nanoscale innovations are deployed to develop micro-scale models, such as soil constitutive models. However, for such transition from nano- to micro-scale and 'upscaling', the behaviour of material needs to be simulated at an intermediate range of scale, broadly referred to as the meso-scale. Less established simulation methods are available at mesoscale. An inherent challenge to mesoscale simulation is the hardship of simulating long timescale (or slow) processes that may originate in such intermediate scales, like creep, fatigue, reaction rates and hydration. In other words, it is incredibly hard to model large timescales in small length scales [8]. Mesoscale models then inform microscale models, such as constitutive soil models, which are then extrapolated to engineering properties and capitalised for the benefit of geotechnical and petroleum engineering applications. The thermodynamic perturbation method is gaining interest at mesoscale [9-10]. Alongside with MD simulation, the two methods combined are offering a chance to study interactions of multiple platelets with varied orientation (Fig. 2), and a fresh insight into clay platelet arrangements – hence clay microstructure, aggregation under progressive pressure, and evolution of elastic stiffness and anisotropy with size of platelets.

Moving upwards along the scale and for sands, the surface area becomes small relative to the overall volume or mass of the particles, hence gravitational effects become more significant. The overall behaviour of the material for sands is insignificantly influenced by surface interaction and charges. Instead, the overall behaviour is influenced by the variety of particle shapes, size, sorting, and surface topology that can be as complicated as the topology of mountains. Significance of sand behaviour manifests in consequences of its problematic behaviours, including softening, flow and liquefaction. Examples of liquefaction ramifications include the wide-scale destructions in the Maria District, San Francisco, after the 1989 Loma Prieta Earthquake, in Onahama Port, Japan, and in Shortland Street in the suburb of Aranui, New Zealand, in 2011. The "Tesco" Tunnel collapse in June 2005 in London, UK, that incurred an estimated cost of £8.5 million is another notorious example. More recently, in January 2019, the failure of Minas Gerais tailing dam in Brazil claimed 157 lives and showed the catastrophic significance of problematic sand behaviour.

Fig. 2 Qualitative picture of aggregation during MD simulations; Clay platelets' orientations according to the φ angle (0° representing alignment of normal vector of platelets with the *z* axis) [14]

Understanding how to work with soil has consequences, both in terms of natural hazards that are stemmed from soil's highly complicated behaviour, and in terms of urban environment and construction of surface and subsurface structures that are surrounded with soil. It is highly advantageous to draw in expertise from other areas and disciplines in developing the understanding of soil, and its inherently complicated behaviour that is also dependent on the environment. These include research in particuology, powder technology, pharmaceutical sciences, and food and process engineering. A good example is the recent studies on fragmentation of infant milk agglomerated powder during transportation, including how inter-particle collisions play more significant role relative to particle-wall impacts during transportation (Fig. 3), and lessons for understanding soil particle crushing [11]. Another engineering discipline that can better shape knowledge of soil at fundamental level is metallurgy. An example is recent advances of in-situ synchrotron radiography, discrete element method (DEM) simulation and thermographic imaging (Fig. 4) that show the resemblance of semi-solid alloys to granular materials. In this context, [12] brought concepts of critical-state soil mechanics (CSSM) and shear-induced dilatancy that occurs in dense sands into the metallurgy discipline. They showed an improved understanding of dilatancy – this assisted in identifying weak zones in semi-solid metals that are used to cast mechanical components. More recently, [13] adopted the CSSM framework for interpretation of triaxial shear data of semi-solid alloy and reported similarities to soils in terms of the pressure-dependent flow stress and pressure-dependent volumetric response.

Fig. 3 Simulation of uniaxial compression of highly porous particulate matters through importing the "diffusion-limited aggregation" algorithm into 3D DEM software package PFC3D [11]

Fig. 4 Left: aluminium die casting and significance of identifying areas of potential weakness [15]; Right: coupled LBM-DEM simulations and time-resolved synchrotron X-ray radiography applied to the study of complex stress–strain behaviour of globular Al–Cu alloys and links to critical-state soil mechanics [12]

2.2 Challenges in Predicting the Behaviour of Soils

An informed adoption of simulation and observation methods for soil needs an in-depth understanding of the difficulties in predicting the behaviour that arises from the fact that soil is a particulate material. A natural (not engineered) soil is generally inherently variable. This differentiates soil, as a material to work with, from most other engineering materials. It is intuitive to geotechnical engineers that soil strength is stress-dependent, and the extent of steady states depends on soil packing state. The non-linearity of stiffness and the fact that stiffness is also stress dependent are other phenomena intrinsic to a granular material and which make prediction of soil behaviour more complicated. However, this is not limited to natural soils, but arises from particle-scale interactions. As the contact force increases due to an increase in the confining pressure, the contact area increases and hence the stiffness. Furthermore, stiffness progressively degrades with increasing strain, a fact that arises from the particulate nature of soils. Other challenges of working with soil include the hysteresis under cyclic loading, strain softening and localization, anisotropy and significance of intermediate principal stress, phase transformation under undrained loading, non-coaxiality [14], and temperature-dependent properties [16].

2.3 Models, Simulations and Methods

Many of the biggest challenges regarding ground engineering are associated with fundamental behaviours of soils. Taking coarse soils as an example, these include grain-to-grain interactions, the influence of pore space, and dilatancy. Particle-continuum duality of soils suggests that all behaviours which we can model at the macro-scale stem from the physics at the micro- or granular-scale. The ground, which we see as continuous from afar, is fundamentally composed of distinct grains separated by pore space. Tools such as micro-computed tomography (μCT) and scanning electron microscopy (SEM) that facilitate visualization of the particulate, or granular, nature of soils allow us to visualize the efficacy of different ground improvement techniques at the micro-scale. For example, [17] used SEM coupled with energy dispersive X-ray spectroscopy as a tool for evaluating the capability of coal ash treated with microbial-induced calcium carbonate precipitate to minimize leachability of trace elements into groundwater sources. Other imaging tools, notably X-ray μCT, facilitate visualization of grain movements and interactions in three dimensions (3D) during shearing (e.g., [18-20]). This section will explore advances in numerical and observation methods and technologies, and how these are offering novel insights into soil as a complex particulate matter.

2.3.1 Advances in Simulations

Modelling and simulation, in the context of NiSE, aims for betterment of our understanding of the origin of material behaviours, extrapolating long-term behaviours, designing composition and microstructures, in-silico design of complex materials, and new ways to minimise infrastructure degradation and maintenance, as well as to increase resilience.

Nanoscale: Molecular Modelling

Simulations at nanoscale offer an understanding of atomistic-level geochemical processes required for identification of mechanisms and properties that control the thermodynamics and kinetics of soil in its natural, weathered and mediated forms. In the context of NiSE, nanoscale modelling provides a broad range of opportunities, including predication of dissolution, precipitation and reprecipitation rate of biomimetic and biogenic materials (e.g., biopolymers and how these interact with phyllosilicates in the short- and long-terms), biocrusts formation, evolution and degradation, and formation of Calcium Silicate Hydrate (C-S-H) in deprotonated clays. These provide the basis for prediction of complex materials' behaviour. Noteworthy among several textbooks that provide comprehensive reviews of molecular modelling methods is [21]. Molecular mechanics is a common thread and includes a range of techniques, including MD simulation, which has received considerable interest in the geoscience discipline. The MD technique computes forces, based on Newtonian physics, to evaluate the time evolution of a system on the time scale of pico- and nano-seconds. Recent uses of atomistic simulations in the context of NiSE include development and testing of hybrid nanocomposites of C-S-H with organic compounds, and also composites (from intercalation of biomediated or bioinspired materials into clays [22]), modelling the interactions between calcite and organic matters (kerogen) within the soil pore phase and implications on calcite-kerogen binding [23], and validating efficiency of plant-microbial combined bioremediation of PCN-contaminated soils [24]. Figure 5 presents examples of molecular simulations. In Fig. 5a, outputs from MD analysis are presented, aimed at determining chemical interactions between kerogen and calcite within the nanoscale voids of a porous soil, and measurement of interparticle forces. Fig. 5b presents outputs of MD analysis using Large-scale Atomic/Molecular Massively Parallel Simulator (LAMMPS) package to study creep deformation of C-S-H. The method simulates the artificial aging observed in granular materials subjected to vibrations. Figs. 5c,d show crystal structure and forcefield for a complex multibody nano-silica (NS)–kaolinite–sulphates system. Synthetic NS replicates weathered quartz in the sedimentary environment and, hence, in the context of NiSE, counts as a bio-inspired material. Fig 5c illustrates the process of silicatisation of kaolinite (soft clay), where orthosilicate anions share electron with the edge oxygen atom of aluminium octahedral unit to form strong Si-O-Si-O rings [25]. Fig 5d illustrates the NS–kaolinite–sulphates system determined by the summation of all energy interactions over all atoms of the system [25], and formation of Al-HO-Si-O-Si-O-M-Anion and Al-HO-Anion-O-Al-O rings that assist retaining the intra-lattice pore spaces (an objective in NiSE).

Fig. 5 Examples of molecular modelling and their application in geomechanics in the context of NiSE: (a) molecular dynamics (MD) simulation of minimized and equilibrated kerogen–calcite system that is useful for calculating the non-bonded interactions between the organic matter and calcite in porous soils ([23] – with some modifications); (b) variation of shear strain (creep) with potential energy against number of loading/unloading cycles in C-S-H [26]; (c-d) crystal structure and forcefield for a complex multi-body NS–kaolinite–sulphates system [25]

Mesoscale: Particle-based Simulations

Particle-based simulation, as one of the many possible bespoke mesoscale simulation techniques, offers upscaling from molecular simulations. It summarizes many hundreds of particles as a single particle and reduces the degrees of freedom to make simulations more efficient. The technique is particularly useful in determining the behaviour of aggregated nanoparticles of various shapes and morphologies – many kinds to be described later in this contribution – after aggregation. The technique allows extracting properties from the nanoscale and upscaling these into actions at microscale. For example, the method can average out interaction potential between molecules into potentials of mean force between particles, thereby allowing an insight into static and dynamic mechanical behaviours of aggregated nanoparticles. The technique has gained much recent interest and is being refined to avail achieving long timescales, and also to accommodate less simplified and more rigorous chemical kinetics and reactions [8]. The latter allows better imitation of formation and degradation of materials.

Three examples of mesoscale simulations, within the context of NiSE, are the application of chemo-mechanics mesoscale simulation to study the rate and mechanisms of agglomeration of nanoparticles and C-S-H precipitation [27], the recent study of self-organisation of minerals and bacterial activities during MICP – microbial-induced calcite precipitation [28], and the recent use of Kinetic Monte Carlo (KMC) to simulate removal and insertion of particles into aggregation of particles (connected together with an effective interaction potential) in order to model dissolution and precipitation [29]. The latter work marks integration of chemical-transformations in particle-based simulations and could be of interest to researchers studying bio-mineralisation and self-healing at mesoscale, and also carbon sequestration into silicates and carbonates.

Microscale: Discrete Element Method (DEM)

The Discrete Element Method (DEM) continues to gain popularity as a strong tool in capturing, arguably, all challenges in predicting soil behaviour [14] at the micro-scale. DEM idealises soil grains with geometries that can be described analytically, allowing creation of contact/rheological models. In DEM simulations, assemblies of spheres are most common, where the spheres are rigid and allowed to overlap by a small amount. The overlap is then used to calculate the magnitude of the normal interparticle force, through normal springs that can be linear or non-linear. In the shear directions, particles are allowed relative movement to mobilise shear force, which may come up to a threshold value at which particles begin to slide relative to each other. In this, the DEM method allows contacts to form and to break. DEM is an *abstraction of reality* and a method that allows creating virtual samples of soil (sand), running simulations, and measuring the forces between individual particles. Despite the popularity of this method in the geomechanics discipline, the big limitation of DEM is the number of particles that can be considered. For instance, a 1 cm^3 box of sand contains approximately 150,000 particles (of uniform size and 200 µm median diameter). The majority of simulations published in leading geomechanics journals report findings from simulations using less than 150,000 particles in response to computational costs — that is, hardly a reasonable representative element volume. This can negatively impact the boundary effects in materials behaviour [30]. The constraint has been partially relaxed in recent years through using novel codes and high-performance computing.

An important example of DEM advantage in understanding the behaviour of open-structured particulate matters is the impacting of fines fraction on seepage-induced boiling and flow (static liquefaction) potential of porous granular soils. Hydromechanical soil properties, such as air entry value, collapsibility, and potential of flow, are associated with the overall layout of interconnected micro (<0.001 μm), meso (0.001 to 0.25 μm and 0.3 to 1.5 μm) and macro (2 to 20 μm) voids, and the degree to which these contain fines at any one time [31-32]. These 'fractions' of void spaces control soil packing states [33]. For example, a Random Loose Packing (RLP) that typically occurs at void ratio above 0.6 changes to Random Close Packing (RCP) as void ratio reduces to typically between 0.5 and 0.6. Under constant effective stress, such change in void ratio can occur as a result of fines migration. Changes in void ratio can also be produced as a result of mineral dissolution and/or biodegradation [34]. In the context of NiSE, fines can be additive nuclei. [35] found a threshold 30 to 40% fines content, at which point idealised skeletal and fine void ratios reach to a similar value [32]. This marks a state where an interconnected homogeneous network of pores form and the soil reaches the phase transformation stress state (static flow), which is an unwelcomed condition (Fig. 6). DEM simulation allows quantification of the degree to which fines carry effective stress and their ability to move through the pore network (Fig. 7 – [36]).

Challenges of DEM

One of the greatest challenges in numerical simulation of granular materials and soils is the number of grains in a simulation. A standard triaxial test sample of cohesionless sand could have millions of individual grains, which is a prohibitive amount for a single-core computer. Inclusion of complex grain morphologies increases the computational demands of a single simulation. Even with simplifications in terms of larger grain sizes and idealized grain shapes, simulations of boundary-value problems involving granular materials requires advanced computing tools. For example, earthquake surface-fault rupture has been simulated with hundreds of thousands of grains with multi-core processing (e.g., [37-38]) and with graphics processing units (e.g., [39]). Upscaling the number of grains to the millions is achievable with high performance computing (e.g., [40-41]). As processing units and computational technologies improve, increasingly complex simulations of soil behaviour become possible, thus facilitating deeper understanding of soil behaviour at the granular-scale.

Fig. 6 For threshold fines content of 30 to 40%: (a) maximum static flow potential [45]; (b) equal idealised micro- and macro-void ratios [35]; (c) changing fabric from RLP to RCP as fines content increases beyond the 30 to 40% threshold [32 – with permission from ASCE]; (d) maximum liquefaction risk [35]

Fig. 7 DEM–DFD coupled simulation for a gap-graded material showing the greater ability of fines to transmit effective stress through the pore network [36]

Level-Set Discrete Element Method (LSDEM)

In order to more fully understand soil behaviour at particle level, the contacts between grains and other materials must also be quantified. Except in the case of photoelastic materials, high-resolution imagery typically will not offer any information on the magnitude of forces that act between grains. Numerical modelling is necessary to quantify these contact forces in terms of contact orientation and contact force magnitude. DEMs are highly suited for contact force calculations based on Hooke's law for elastic springs. In particular, the level-set discrete element method (LSDEM, [42-43]) can capture the exact morphologies of grains observed in µCT images, as well as quantifying the contact forces acting between contacting grains. LSDEM coupled with µCT allows for the shapes and kinematics of the grains themselves, and the distribution of contact forces that exists within the granular matrix, to be quantified fully via one-to-one physical–numerical comparisons. Entire shear simulations are possible for complete analysis of CSSM within the shear band itself (e.g., [43]). Furthermore, more complex granular mechanics, such as grain fracturing and crushing, may be included to evaluate the critical state behaviour of soils at a wider range of stresses (e.g., [44]). This level of detail in simulations can improve soil constitutive models by providing a means of virtual laboratory testing.

Critical State Soil Mechanics (CSSM) for Reinforced Soils

[46] are among the few who have performed high pressure laboratory studies on fibre-sand mixtures and adopted a critical-state framework to describe their mechanical behaviour. [47] conducted dynamic and monotonic triaxial testing to study the behaviour of carbon-fibre-reinforced recycled concrete aggregates by focusing on the very small and large strain ranges. Authors reported that, at large strains, reinforced and unreinforced specimens showed comparative stress–strain response and volumetric behaviour with similar critical state parameters, the fibre-reinforced specimens having slightly higher critical state angle of shear strength. More recently, [48] utilised critical-state framework to compare the performance of polypropylene and rubber fibres in well-graded

decomposed granite. In a similar study, [49] examined the effect of adding fibres to a completely decomposed granite (CDG) in the context of critical-state framework. They reported that while unreinforced CDG is sensitive to sample preparation, the reinforced soil is not sensitive to the method of material or sample preparation. It is evident from earlier studies that, until now, not many have attempted to investigate the CSSM for fibre-induced cohesive soils.

Soil constitutive models for reinforced soils

Although several studies have been conducted on fibre-reinforced clays, little is known on the implications of in-situ compaction of cohesive material reinforced with fibres. [50] presented findings from a study of the compaction of clay peds and fibres, and the consequent creation of discontinuities in the contacts between clay peds and clay-peds-and-fibres.

In their extensive study of Lambeth group clay, [51] reported that a large amount of the formation comprises of largely unbedded, mottled silty clay and clay alone. They reported that during the deposition of the Lambeth group, fissures with polished and slickensided surfaces developed due to desiccation throughout seasonal changes in ground moisture. [51] also studied the effect of fissuring on compression behaviour of over-consolidated Lambeth group clay and showed that the compression response of tested specimens is highly dependent on fissures. In a later study, [52] reported that there are two state boundaries in London clay not subjected to previous shearing; that are the upper bound, defined by the peak failure envelope of the intact clay without fissures, and the lower bound given by the parameters defining the strength of the fissures.

London Clay belongs to a geological unit above the Lambeth Group and they have similar characteristics; however, the former has been deposited under a variable sea level, with sand lenses found when the sea level was shallow, causing the appearance of beaches. London Clay is highly over-consolidated, intensely fissured. [53] and [54] showed that the effective strength of London Clay with dull or shiny surface fissures exhibit a zero effective cohesion on fissured surfaces and an effective friction angle equal to the global soil substance of the intact material, whereas slickensided surfaces show an effective strength similar to the residual values. More recently, [55] studied the influence of the structure on the behaviour of London clay. They used the State Boundary Surface (SBS) concept, which is constructed from all the effective stress paths for normally consolidated clay, lightly consolidated clay, over-consolidated clay and heavily over-consolidated clay at different initial stress states and for different test conditions (drained and undrained), to identify the changes in structure. They stated that, in compression, the peak state of clay from different units plot significantly above the SBS from the reconstituted specimens (i.e., SBS*) for isotropically consolidated samples; this was considered a feature of the natural structure of the clay. [55] discussed the implications of structure increasing with depth; this remains a matter of debate.

In a study on a similar highly fissured and structured clay, [56] reported that the SBS of the unfissured clay is larger than that of the reconstituted clay, while the SBS of a clay with a high fissure intensity is smaller than the same reconstituted clay. The authors further suggested that the intense fissuring degrades the mechanical properties of the clay, with respect to both the original unfissured material and the reconstituted soil. [56] reported that the fissured material had fissures with matt surfaces, where the peak strength of the clay generally stayed above the critical state. Additionally, [56] and [57] found that due to the heavily sheared and slickenside-like nature of the surface of the scales, the peak strength of the natural soil is lower than the critical state of the reconstituted soil.

2.3.2 Advances in Spectroscopic Methods

Microcomputer Tomography (*μCT*)

Microcomputer tomography offers high resolution images of sub-cores obtained from soil samples impregnate with epoxy resin. In a seminal recent study, a series of radiographs are obtained as soil samples are rotated in front of the X-ray source to generate 3D images. Figure 8 of this paper presents a rare and useful view of the μCT setup. The technique is continuously developing, not just in terms of the technology around acquiring the images, but in the ability to analyse the data that emerges.

Fig. 8 Typical microcomputer tomography laboratory setup [14]

An important application of μCT in the context of NiSE is an improved understanding of double porosity, which is an intrinsic quality of bimodal soils (e.g., silty sands, mediated sands with nanomaterials). For bimodal soils, the size, geometry and evolution of constrictions or pore throats play pivotal roles in soil behaviour. Constrictions form the boundary between various scales of pore spaces and their reliable measurement, as a grain scale quality, can inform a number of problems across the spectrum of porous particulate matters. A simple example is a recent study on Reigate sand from south of London, UK. Reigate sand has a self-supporting quality in open cuts, as particles naturally interlock and come together like jigsaw pieces. [58] conducted drained triaxial compression tests on intact and reconstituted samples at a constant 0.48 void ratio and under a constant 300 kPa cell pressure. They showed the intact material exhibits much more strain-softening and a higher peak than the reconstituted material. Using the μCT, they plotted contact index (i.e., the ratio of particle contact area to particle surface area) volumetric distribution for the two materials to quantify the contribution of contacts at particle scale. In addition to particle interlocking, constriction-size distribution informs on how, and if, fines migration through the pore network modifies the contacts and impacts the skeletal stresses, suction, stiffness and steady states. For example, [59] used DEM to explore the impacting of particle-size distribution, relative density, and coefficient of uniformity of filters (i.e., porous granular soils) on constriction size distribution (CSD). They did not just test the viability of characteristic diameters in assessing filter retention capacity, but also the likelihood of fines entrapment in narrow void throats. [60] exhibited the benefits of using network modelling (specifically the 'random walk' model) alongside CSD analysis to simulate the migration of fines through the soil pore network (Fig. 9). They used CSD data to confirm an earlier experimental finding of [61]; that is, the size of constrictions rather than topology of pores controls movement of fines through the pore network. In the context of NiSE, µCT-DEM and µCT-Network Modelling assist in CSD-informed design of sands stabilised with a range of additives (from biopolymers to colloidal NS) in their naturally-high original porosity. These also help a better understanding of seepage implications in flood defences and earth-based water reservoirs that are built with open-packed granular soils.

Fig. 9 (a) Example of a network model for simulating the migration of base particles (e.g., clay, nano-stabilising agent, biopolymer nuclei) through the network, where the size of the edge of the network is determined from CSD, informed by µCT [60]; (b) Criteria, whether a base particle would move through the constriction, whether it would be trapped, and when it would be retained in the void space [60]; (c) An example of determining CSD as a function of 15% percentile of particle size [59]

The types of quantifiable interactions observed via µCT are not limited to soil grains. Complex biological processes that occur within the soil may also be visualized. µCT has been used to study the interaction of root growth with soil, and how root growth affects water uptake [62]. It has been used to study soil response due to ice formation in pores during freeze–thaw cycles [63]. These processes involve complex interactions with the grains themselves and the pore space between the grains, and are practically impossible to be studied in absence of advanced imaging tools. µCT has also been used to study the interaction between rigid and soft particles in sand–rubber mixtures as a means for improving the properties/behaviour of sands [64]. Not only can the grains be visualized via processed X-ray images, but the kinematics and interactions of the grains can be quantified using software, such as the python-based Software for Practical Analysis of Materials (SPAM, [65]). This allows for shear-induced deformations to be visualized via grain rotations, grain displacements, shear strains, and volumetric strains, all in 3D. All experiments using this technique are performed in "miniature" simples. However, the gain in resolution comes at the cost of losing the size of the representative elementary volume (REV).

Particle Image Velocimetry (PIV)

The PIV technology – also known as digital image correlation (DIC) – allows non-invasive measurement of soil deformation by tracking the movement of individual soil particles through consecutive images captured from soil samples (test specimens). For example, [66] deployed the PIV technique to contrast horizontal and vertical deformations of a model slope, before and after modification with waste carpet fibres. More recently, [67] assembled a PIV strongbox on a standard beam-centrifuge to visualise flow and understand its mechanisms as test penetrometers were driven into a sequenced clayey soil (Fig. 10). There is scope for use of this technique in tracing the displacement of fines through the soil pore network.

Fig. 10 Soil flow mechanism as a T-bar penetrates stiff clay and pushes through an underlying soft clay stratum – D_t is the bar diameter; d is its vertical displacement and x is its horizontal displacement [67].

X-ray computer tomography (CT) imaging

In the NiSE context, an insight into microstructural evolution of porous soils under loading conditions benefits the design in a number of ways. The X-ray CT imaging technique allows real-time capture of soil pore spaces in 3D under triaxial loading. For soils reinforced with fibres (natural or engineered), the technique offers a chance to capture, at sub-micron resolution, the evolving orientation and tortuosity of reinforcing fibrous matters within the spatial domain of soil under stress. This is valuable information, offering a unique chance to explain the, thus far, controversial anisotropic behaviour of fibre-reinforced soils [68-69]. In a quite innovative recent attempt, [70] managed to build and instate a miniature triaxial cell inside a Zeiss Xradia XRM520 Versa X-ray CT machine (Fig. 11). Typical outputs of CT results are illustrated in Figure 12.

Fig. 11 Interior of the X-ray chamber accommodating miniature triaxial cell [70]

Fig. 12 Reconstructed 3D greyscale images of triaxial mini-specimen at three axial strains and three views (XY, XZ and 3D), followed by spatial distribution of fibres and 3D distribution of fibre orientation and length at three axial strains (reproduced from [70])

3. Advances in Materials

An emerging sub-discipline in geotechnical engineering is bio-geotechnical engineering that includes two streams of processes; these are bio-mediated processes, where interventions are directly managed and controlled through biological activities and living organisms; and bio-inspired processes, where interventions are abiotic, and designed to be inspired by biological principles. The latter is also often referred to as nature-inspired abiotic processes and involves the use of non-living organisms. Core objectives of biogeotechnological interceptions are, first, to accelerate beneficial organic and biologic processes to occur in a time frame of interest, and, second, to induce adverse processes in a context where the effect is beneficial [71]. This sub-discipline often appears in literature under Nature-Based Solutions (NBSs) that refer to technologies and materials used to preserve and sustainably manage the ecosystems, and also to restore ecosystems' degraded functions.

3.1 Bio-mediated Materials

3.1.1 Deep-rooted vegetation

Use of vegetation for stabilisation of earth structures, including infrastructure and natural slopes, has attracted much interest in recent years. The emphasis in the past few years has been on understanding the role of vegetation in the context of the slope–vegetation–atmosphere interaction through cutting-edge field monitoring and testing. [72] presented a recent important state-of-the-art review on impacts of climate change in the context of engineered slopes for infrastructure. The work offers a European perspective and is written by members of COST Action TU1202.

Other recent pivotal contributions include field survey of desiccation cracking of clay-fill embankments, with reference to atmospheric and soil–hydrological specific conditions ([73] – Fig. 13a). [74] deployed a Fortran95 powered two-dimensional slope stability model with hydrological and vegetation effects, SSHV-2D, to incorporate evapotranspiration-induced temporal and spatial distribution of water content on the mechanical effects of the vegetation and overall implications on slope stability [74]. [75] studied the impact of selected deep-rooted vegetation cover on the hydrological balance at the ground surface. [75-77] reported on a 3-year monitoring programme of surficial desiccation cracking, piezometric-head fluctuations, soil matric-suction levels and hence shear strength as part of a crop test at the toe area of the Pisciolo ([75-77] – Fig. 13b). The Pisciolo landslide was deemed to follow a slow and deep weather-induced mechanism. As such, [75] considered the vegetation layer only in terms of hydraulic reinforcement (i.e., evaporation and transpiration rates). The team reported on seeding several deep-rooted crop types belonging to two vegetation families: the *leguminous,* belonging to the "C3 carbon fixation" type [78-79; 174-175] (Fig. 13c), and the *Gramineae,* belonging to the "C4 carbon fixation" type [80-81] (Fig. 13d). Such crop families differ basically in leaf structure and consequently biological activity and in the vegetation life cycle [82]. In particular, the C4-cycle crops are generally referred to as evergreen plants, as they exhibit high photosynthesis potentials and water retention capacities [83].

Fig. 13 (a) BIONICS research embankment, in northern England, covered to the north with grasses (e.g., *Alopecurus pratense* and *Lolium perenne*) and to the south with wildflowers (e.g., *Leucanthemum vulgare*, *Filipendula ulmaria*, *Achillea millefolium* and *Knautia arvensis*). Instrumentations allow measurement of volumetric water content, electrical conductivity and soil temperature [73]; (b) Pisciolo hillslope in southern Italy covered with (c) C3-cycle *leguminous* and (d) C4-cycle *Gramineae* plants [87]

The C3-cycle crops are not able to control the stomata closure, such that water is likely to exit the plant system in the form of water vapour [82], causing the plant to eventually wilt. With reference to the monitoring data of the Pisciolo test site, [75] reported preliminary data of the impact of selected deep-rooted vegetation on the soil state at depth. In particular, the vegetation has been seen to act as a heat filter, reducing temperature fluctuations in the subsoil, with reference to spontaneous and sparse vegetation. [75] reported lower orders of the water content in soil throughout the year up to 1.6 m depth, as compared to soils covered with spontaneous vegetation. Hydraulic conductivity and retention properties of the soil appear to be strongly impacted by the root system of the selected vegetation [84-86]. In particular, published preliminary monitoring data suggests a one order of magnitude increase in the saturated hydraulic conductivity for the rooted soils, compared to unrooted soils. The water retention capacity of rooted soils appears to resemble those of coarser soils. This is manifested by the significant lower orders of air-entry value [75].

3.1.2 Biocement

By 2016, there were some 2400 publications on 15 types of biocements across a spectrum of disciplines, including microbiology, enzymology, biogeochemistry, and mineralogy of biocementations [88]. Examples of natural biocementation signatures on earth include sandstones and are brought in Fig. 14.

Biocements are generally used in the construction industry, where there is a need for a low-viscosity cementing solution for filling pores through injection, or to control soil erosion and dust deflation through spraying. However, these are generally more expensive than traditional cement, costing between 200 and 250 US$/t. This is above 100 US$/t, the approximate present maximum cost of novel materials for economic viability [88].

Fig. 14 Signatures of natural biocementation in sandstone: (a) Bryce Canyon National Park, Utah, USA [89]; (b) Arches National Park, Utah, USA [90]; (c) The Belogradchik, Vidin, Bulgaria [91]

Biocements contain two-to-four components: (1) a main structural component which can include salts of Ca^{2+}, Ca^{2+} and Mg^{2+}, or Fe^{3+}; (2) a pH-controlling component, that can be urea, nitrate, phosphate, acetate, or formate; (3) a bio-controlling component, that can be specific microbial cells or enzymes; and (4) a biopolymer to form the 3D structure of biocement and improve the overall mechanical properties [92]. A limitation common to the vast volume of published works on this topic is little insights from expert biotechnologists. Effective design of biocements require inputs from biotechnologist with expert knowledge of microbiology and biochemistry, alongside civil/geotechnical engineers. One of the most recently developed biocement types is Hydroxyapatite [93], a product of bones from meat-processing wastes, that can be used in conjunction with elastic biopolymers to diminish brittleness.

3.1.3 Bacterial Biofilm

Bacteria rarely grow as unicellular planktonic cultures. Instead, bacteria predominantly exist as communities of sessile cells in the form of biofilm [94]. Biofilms (Fig. 15a) are structures comprising microorganisms surrounded by a matrix that allows their attachment to inert (e.g., soil particles) and organic (e.g., mucosa) surfaces. They are a product of bacterial transition from the unicellular (planktonic) life phase to multicellular (sessile cells). Once attached to surface, they multiplicate and begin to produce/exude extracellular polymeric substances (EPS), which assist them to form bacterial colonies. Growth of colonies does not last forever; these break up via desorption, detachment or dispersion, releasing bacteria and biogenic gas back to the surrounding medium. In the case of soils, this medium is the soil pore space. Bacteria may fill pore spaces or form inter-particle bridge and buttress connectors, or may clog pore throats, or coat soil particles (soft viscous biofilms) – Fig 15b. Bacterial biofilm are soft, viscous, ductile, and elastomeric. They enhance damping and small-strain stiffness of soil.

Two examples of benefitting from biofilms in sands are presented here.

[95] compared the impact of two different microbial biofilms — from multiplication of *Shewanella oneidensis* (MR-1) and *Pseudomonas putida* bacteria in a cocktail of Triptic soy broth, sucrose and phosphate buffer — on the behaviour of Ottawa 110 sand. They reported a sharp, substantial and rapid decrease in permeability (unwelcomed in the context of NiSE), no change to the compression P-wave velocity (measured by piezoceramic transducer) over time, an increase in shear S-wave velocity (measured by bender elements), no change to P-wave peak-to-peak amplitude and, hence, the pace of seismic waves attenuation. To this end, both biofilms attenuate seismic wave propagation at the cost of decrease in permeability. The second important recent contribution is the work of [96] on growing bacterial Dextran in clean sand. They grew an aerobic bacteria, *Leuconostoc mesenteroides*, in a cocktail of yeast extract, sucrose and phosphate buffer to generate a viscous Dextran biopolymer (Fig 15c), coating sand grains. Dry sand mixed with bacterial culture was compacted in layers to reach a compacted void ratio of 0.6, with monitoring of the geophysical properties of the mediated sand performed over the following 41-d period. They showed no changes to the shear modulus and stiffness over time, a progressive decrease in permeability, welcomed decreases in P- and S-wave peak-to-peak amplitudes — indicating a faster attenuation of waves, decreased wave propagation, and a medium that better conveys seismic waves.

3.1.4 Biological Carbonate Precipitation Technologies (CPT)

Carbonate precipitation technologies (CPT) began to gain interest from the early 21st century, offering a spectrum of applications, including solid-phase capture and remediation of problematic trace metals and radionuclides [97], remediation of fractures in concrete [98], carbon sequestration [99], and improvement of soil and fractured rock. Biological CPT or managed precipitation of calcium carbonate through ureolysis fits both bio-inspired and bio-mediated ground remediation techniques and has potential to seal porosity and/or to enhance soil steady states at an almost unchanged macro-scale void ratio. Urealysis occurs through the hydrolysis of urea to ammonia (NH_3) and carbonic acid, subsequent equilibrium in pore water and formation of bicarbonate, ammonium (NH_4^+), and hydroxide (OH) ions. The elevated pH from OH^{-1} ions and abundance of bicarbonates trigger precipitation of calcium carbonate – preferentially calcite polymorph [100]. However, the technique is mainly only applicable to fine sand or coarser soils. Recent work by [101] casts doubt on the appropriateness of using standard sands (e.g., Ottawa 20-30) for biological CPT-treatment trials and geomechanical testing. This shows the importance of full-scale (field) trials that, to date, have largely failed to attract much interest – due to costs, quality assurance, quality control, possible environmental impacts, and logistical constraints. The implications of the toxic ammonium chloride by-product of ureolysis continues to be a concern [102]. To bring this into context, using CPT treatment for sealing of a 100 m (L) by 5 m (W) by 2 m (H) dam can pollute about 4.5x10^6 m^3 of drinking water and 100 km^3 of air [103].

Fig. 15 (a): Bacterial life cycle and biofilm formation [94]; (b): possible forms of bacterial growth on soil particle surface [104 – with permission from ASCE]; (c): clean Ottawa sand ($D_{50} = 120\ \mu m$) packed to a void ratio of 0.6 (left), transformed into Dextran-mediated sand (middle), where particles are coated and bridged at the cost of a decrease in porosity, and hence permeability [96]

Microbial-induced carbonate precipitation (MICP)

Bacteria are abundant in soil; for instance, in one gram of soil in top 1 m, there are approximately 2x10^9 bacteria, many of which can survive and thrive at deeper depths. Over the last decade, there has been increasing attention over what microbial processes can offer to geotechnical engineering [105]. MICP is a biomediated process for precipitation of calcium carbonate [100], desirably at particle contact points. In MICP, microbes produce the urease enzyme. *Bacillus pasteurii* – also known as *Sporosarcina pasteurii*, an alkalophilic bacterium with a highly active urease enzyme – is a microbe type commonly used in MICP via bioaugmentation [106]. Important field trials include the stepwise approach devised and implemented by [107]. Figure 16a shows the 0.9 m x 1.1 m x 1 m sand box that received 3500 litres of bacterial suspension and 0.5 M urea/$CaCl_2$ reagent solution in 8 intervals and over a 50-d period. Scaling up from 1 m^3 to 100 m^3, Fig. 16b shows an 8.0 m x 5.6 m x 2.5 m container filled with saturated, loose poorly-graded medium siliceous sand (average dry unit weight of 15.6 kN/m^3) built by [108] for a large-scale trial. A cocktail of highly ureolytic bacteria suspension and urea/$CaCl_2$ reagent solution was injected sequentially, through three 300-mm dia. PVC injection wells at 1 m spacing, and pumped towards three extraction wells at 5 m distance over a 16-d period. Moving towards full field-scale, [101] treated 1000 m^3 of soil at depths of between 3 and 20 m below ground level by injecting 200 m^3 of bacterial suspension and 300 to 600 m^3 of urea/$CaCl_2$ reagent solution (Fig. 16c). Commercially, a handful of contractors use the technique as a means of ground improvement for subgrades and retaining structures (Fig. 16d). A limitation of MICP, particularly in soils with small pore throats, and in the context of NiSE, is the possibility for bacteria to be physically strained in the soil media causing porosity reduction due to biomass clogging [113]. This is manifested in the X-ray CT scan in Fig. 17, illustrating the spatially resolved maps of the changing porosity throughout and after the MICP process [109].

Exploitation and biostimulation of native microbes continue to attract interest across ecological, quaternary geology and geomechanics disciplines [110-111]. However, a major limitation to employing native bacterial communities is the need for adding organic nutrients, such as molasses, to enrich the biomass [100] and the likely environmental consequences, such as eutrophication. A thorough review of biogeochemical processes in the geotechnical context is given in [112].

More recent 'technological development' attempts include the work of [113], who reported on staged injection of a cocktail of bacterial cell (*S. pasteurii*) and urea/$CaCl_3$ solutions, using a pressure head, into two loose medium sands. For about 6% precipitated calcite and through a comparative experimental campaign, [114] proposed two injection cycles, each with aeration during injections and 24-h solution retention period, with a 6-d drained stage between cycles, and for 0.5 M cementation solution. In addition to baseline strength enhancement, the MICP technique has also been investigated as a technology for stabilisation of crustal layers and mitigation of wind-driven erosion. [115] developed single- and double-MICP spray treat techniques for loose medium silica sand and fine-to-medium carbonate sands. They considered a 6-d gap period between the first and the second spray applications and 28 d of curing post spray treatment. Through referring to findings from wind tunnel experiments, they demonstrated the singly MICP-spray-treated crustal sand layer exhibited no dust deflation for simulated 20 m/s winds measured at 20 cm above the treated sand layer surface.

Fig. 16 MICP trials in three scales: (a) cubic meter sand box [102] – photograph from [116]; (b) 100 cubic meter sand box [108]; (c) 1000 cubic meter field-scale mediation [102]; (d) MICP at large scale: MICP-treated 400-mm dia. column by Soletanche-Bachy [117]

The bacterium *E. Coli*. has been engineered to show pressure-responsive behaviour [118], as discussed, in length, in section 3.2.3. This research was recently extended to an attempt to build sand cube samples (Fig 24d), seeded with bacteria and receiving nutrients through multiple and controlled directions [119]. Findings reported in [119] show that influencing factors on the cemented form is not restricted to the form of the cast (and hence topology of the pore spaces in soil – Fig. 24e,f), and also show how the flow of the nutrient medium can create a diverse range of cementation zones.

Fig. 17 3D visualization of the X-ray CT data illustrating the variation in porosity: (a) pre-MICP precipitation; (b) post-MICP precipitation; (c-d) service time under acidic conditions in favour of $CaCO_3$ dissolution [109]

Enzyme-induced carbonate precipitation (EICP)

EICP is a bio-inspired process for precipitation of calcium carbonate to achieve rapid increases in soil peak strength and dilatancy. The urease in EICP is derived from agricultural sources, such as Jack Bean (*Canavalia ensiformis*) meal [120]. A recent attempt by [121] to create columns of improved sand by EICP exhibited an improved UCS of 400 to 500 kPa achieved at approx. 0.8 to 1.7% axial strain.

Moving up the scale, [122] reported a recent large-scale attempt to build a 0.3-m dia. × 0.9-m long EICP-mediated sand column inside a sand box sizing 0.6 x 0.6 x 1.2 (L) m. They injected a cocktail of urea (1.5 M), $CaCl_2$ (1 M), 9900 U/l urease enzyme, and 4 g/l no-fat milk powder in three shots using PVC 1.2-m long tube-à-manchette (TAM). For <3% precipitated calcium carbonate within a 0.3-m dia. cylindrical treatment zone, they reported an achieved UCS of >500 kPa. They estimated the cost of mediation in the range of $US 60 per cubic meter of sand. An EICP column and needle penetrometer test performed in between two subsections of treated column is illustrated in Figure 18.

Microbial-induced desaturation and precipitation (MIDP)

An undesirable side-effect of using EICP is the consequent toxic ammonium chloride by-product. MIDP is another emerging bio-mediated technology, where nitrate-reducing bacteria in the soil are stimulated to produce biogas and biominerals [123]. Nitrate reduction or denitrification is a novel recent alternative method, where a combination of calcium fatty acids and calcium nitrate are used in conjunction with indigenous microbes to precipitate calcium carbonate. The MIDP technique offers a non-hazardous nitrogen gas by-product, and can achieve significant increases in dilatancy, stiffness, strength and cyclic resistance of host sands [124]. The application of MIDP should be designed to result in 1–3% $CaCO_3$ cementation, which requires 25–70 kg/m^3 substrate and application of the cocktail in 3 to 10 flushes.

Microbially Induced Desaturation (MID)

As an alternative desaturation approach, the required substrate to achieve 10–20% desaturation of N_2 by the MID approach would decrease to 0.7–1.5 kg/m^3 – that is, roughly 40 times less substrate required than MICP – and benefits in a single flush application. As such, the MID approach is a significantly cheaper option compared to other biogeochemical options and has relatively benign side effects. The technique was recently trailed at field-scale on sandy and silty soils in Harborton – that is, the area of Oregon’s Critical Energy Infrastructure (CEI) hub – and Sunderland, close to the Portland International Airport, west side of Portland, USA. The main objective of the trial was liquefaction mitigation and enhancement of seismic resistance of local industrial infrastructures that supply over

90% energy of Oregon State. Nutrients (calcium nitrate, or fertilizer, and calcium acetate, or food grade, each 10 g per litre of water) were injected to the ground from a central well and extracted from perimeter wells (Fig. 19a). The denitrification led to the liberation of N_2 and CO_2 gases, which then desaturated the soil to remove the potential of liquefaction. In Fig. 19b, the decrease in P-wave velocity (V_p) is indicative of successful desaturation. The treatment period took one month, and monitoring is ongoing for 3 to 5 years, starting from September 2019.

Fig. 18 EICP trials at field-scale: soil column in box test set-up with TAM and packer, and needle penetrometer measurements done on cemented soil section [122 – with permission from ASCE]

Fig. 19 (a-b) MID test setup in Portland, Oregon, USA: injection probe and monitoring installation, including cross-hole and downhole TREX sensor array measuring excess porewater pressure, V_p and V_s, and CTD divers; (c) measuring fluid volume and salinity, and TEROS-12 sensors; (d) measuring salinity and temperature; (e) P- and S-wave velocity cross-hole measurements [128]

CPT as a means of self-repairing through an autonomous response to damage

Breakage of brittle binding connectors (i.e., bonds) at particle contacts in a porous medium can lead to soils' structural failure. However, once damage occurs and the soil skeleton relaxes to a new equilibrium, the grain contacts might be cemented anew through a *self-healing* ground improvement system that is both responsive and adaptable. Both autogenous (a natural property of the material concerned) and autonomous (an engineered property) systems are able to respond to stimuli, such as bond damage or the presence of deleterious substances (e.g., chlorides in concrete), in order to counteract the problem. Crack formation in concrete has been addressed through self-healing systems which produce grouts *in-situ* and at the location of damage, both biologically [125] and chemically [126], and there is the potential for similar techniques to be applied in grouts for ground improvement. [127] findings demonstrated the concept of self-healing MICP in sand and limestone, where spore-forming bacteria are able to generate a calcium carbonate grout *in-situ*; as the grout forms, bacterial spores entombed in the grout remain until damage occurs, whereupon these spores are exposed and they can germinate, with the resulting cells able to re-heal the damage through further precipitation.

3.1.5 Biopolymer-based soil treatment (BPST)

Whilst most grouts or other bonding agents are strong but brittle, and thus susceptible to fracture in a porous medium, BPST offers a more resilient response to stress concentration. Due to increased ductility, they are able to respond to loading through deformation, rather than brittle fracture. Biopolymers (or natural polymers) are naturally exuded by micro- and macro-organisms (bacteria, plants, etc), and have been shown to affect soil geotechnical behaviour at low levels [129], although this is dependent on environmental conditions (particularly moisture), and biodegradability may limit their durability. However, they are self-sustaining under the right conditions. For instance, biopolymers obtained from inedible parts of cultivated plants have received recent interest as an environmentally friendly grout for ground improvement. [130] collated the application of many common biopolymers in geotechnical engineering. These include xanthan gum (XG) and sodium alginate (SA) [122], guar gum (GG), and mixtures of agar (from red algae) and enzymatically modified starch [131]. Biopolymers are mostly applied to sands, silts and silty sands in less than 2 wt.% [of soil] proportion, and mainly to control the hydraulic conductivity, and also to increase shear strength and stiffness. [132] recently reported on the use of a range of biopolymers for improving Shanghai clay under repeated traffic loading. This is an interesting contribution given the broad range of biopolymers applied to the clay, and it is the first reporting on growth of fungal genus in biopolymer (particularly with casein and carrageenan) treated clays. They reported on the use of carrageenan kappa gum (KG), locust bean gum (LBG), XG, agar gum, GG, SA, chitosan (CH) and gellan gum (GE).

The long-chain structure of biopolymers and certain constituting chemicals (e.g., hydroxyl, ester or amines) supply adhesive forces that help coating and binding of soil particles together [131]. An advantage of BPST over MICP is a better chance of quality/quantity control and the rapid treatment process [130]. Biopolymers are produced from exo-cultivating facilities (Fig. 20), requiring relatively less time and resources (e.g., nutrients, aeration, cultivation environment control). A possible drawback of applying biopolymers on soils, in the context of NiSE, is the consequent elevated temperature, change in soil solution pH, and occupation of the void space [133]. Drivability of biopolymers in soil has remained a practical drawback. To control 'setting time', [134] applied a broad suite of biopolymers to superfine GGBS cement and explored ways to increase the zeta potential of fine grout particles for these solids to remain in suspension for reasonable periods of time in order to allow implementation of the grouting processes.

Fig. 20 Comparison between MICP and BPST processes [123]. Note, in Fig. 20c rods represent soil particles and red-coloured lines represent biopolymer chains, with adhesive force among themselves and cohesive force between them and the soil particles

3.1.6 Deep-rooted vegetation in biopolymer treated clays

A limitation of the deep-rooted vegetation remedial technique is the time required for the growth of plants, and hence for the benefits of the technique to materialise. Injection of a viscous solution of biopolymers can improve the soil strength at the initial state of plant growth, and meanwhile provides carbon, nitrogen and other nutrients needed for plant growth [135].

3.1.7 Fungal mycelial networks

Slipping surfaces/zones in earth slopes tends to develop below the rooting zone, and failure is often triggered by infiltrating rainwater raising the porewater pressure, thereby reducing the effective stresses and degrading the geomechanical properties. Use of deep-rooted vegetation to remove porewater and increase the matric suction, with effects extending below the rooting zone, is fairly well established [136] and was discussed earlier in the paper. Alternatively, infiltration may be minimized via hydrophobic fungal-hyphal networks [137], or rhizosphere-promoted lateral flow [138].

Fungai account for up to 75% of total microbial biomass in soil. Multi-cellular fungi grow in the form of hyphae, forming a complex network known as mycelium. Hyphae are typically 1–3 μm in dia., can have lengths from several micron to several metres (Fig 21a), and they branch out to form complex networks. Mycelia networks are massive, incredibly resilient, adaptable and they have an ability to recover in the face of damage. In soil science, it is widely acknowledged that fungi contribute to soil aggregation and can form soil crusts.

A recent interesting contribution in this field is the work of [137], who reported the first case of water-repellent sand (Fig 21d) created using fungal treatment. They treated sterile sands by growing *Pleurotus ostreatus* (strain M 2191; i.e., edible oyster mushroom) – with and without source of carbon (wood fibres). [139] tested a well-graded sand column of 30-cm high, contained in a Perspex cylinder and with a constant head of water on top, to study the impact of fungi growth on ponded infiltration (Fig 21b-c). The fungal mycelium appeared in the form of a visible, dense network of white tubular elements that prevented water ingress, forcing the water to convey via preferential flow paths. Use of fungi in ground engineering is a new avenue of research within bio-geotechnics and offers creation of a hydrophobic surface layer on erodible sands, reduces infiltration, reduces saturated hydraulic conductivity, and improves the erosion resistance.

Fig. 21 Influence of fungal mycelial networks on soil behaviour: (a) growth of *Pleurotus ostreatus* edible fungi in soil; (b-c) growth of fungi in a column of sand; (d) water repellency [139]

3.2. Bio-inspired Materials

3.2.1 Imitating organic fibrous matters

Natural fibrous matters in soil include certain calcium carbonate polymorphs (e.g., aragonite), reprecipitated carbonates into secondary Ca^{2+} minerals near plant root structures, organic fibrous matters (e.g., fibrous peats), plant rootlets, rhizolithic calcretes [140], and products of carbon sequestration into calcium silicate, dicalcium silicate, tricalcium silicate, tricalcium aluminate and similar hydrated products in urban soils [7].

Fibre-reinforced soil refers to a soil mass mixed with randomly distributed, short, intertwining fibres that imitate organic fibrous matters in form. Fibres are added to soil as standalone matters, or in combination with traditional binders like cement [141].

Opportunities and Challenges

Mixing short fibres with soil is an established ground improvement method for dilative materials (usually granular soils) and is not conventionally considered effective for clays with a low apparent friction angle. However, due to the ease of application and reduced environmental impact, the use of discrete fibres in cohesive soils is gaining interest [142-144]. Effectiveness of fibres is a function of confining pressure. Fibres may compromise strength of sands and clays at confining pressures greater than a critical threshold [145, 46]. Contribution of fibres is more pronounced for lower confinement levels and, therefore, indicative of the effectiveness of the technique in shallow ground [146]. Fibre effectiveness is maximum when soil is subjected to extension and torsion [68]. Fibre surface roughness play a pivotal role in the mechanical performance of fibre mixed soils [147-148]. Treatment of fibre surfaces ahead of soil mixing was reported in [149]. A major technical concern in the use of fibres is the implications of their typical high volume to weight ratio which often disrupts the uniformity of soil–fibre mixtures; that is, high fibre contents may lead to formation of fibre balls and lumps in the treated soil. Furthermore, high moisture contents may lead to fibre floating and heterogeneous soil–fibre mixtures. Distribution and orientation of fibres in soil during service life remain a matter of debate [68,69].

Overall, fibres in soil provide enhanced levels of shear strength [150], decrease residual strength loss [151], mobilise larger strains at failure, increase strain-hardening and reduce deformability, lower shrinkage, and relax implications of soil inherent anisotropy and swelling potential. In laboratory settings, cylindrical test specimens of fibre-reinforced composites typically fail through bulging, rather than shearing along an inclined plane of weakness, indicative of general ductile behaviour.

When introduced to sand, fibres benefit from the ‘rigid wall effect’ to preserve the original open micro- and macro-pore network. This is, however, a function of fines content in the soil [35]. A major concern with fibre-reinforced loose sands is the impact of the difference between stiffness of fibres and mineral solids, and therefore varied interparticle interactions. Figure 22a,b illustrates the first and second stress–strain hysteresis loops for two sands, A and B. In these figures, the dark bold curve refers to clean sand, the grey curve refers to sand with little silt content (known as *Small Silt*), and the light grey curve refers to sand with little silt and 1% fibre. Sand B is relatively coarser, develops larger strains, and a less abrupt, smoother pathway to the flow failure. This is fundamentally due to the better interlocking between particles. Fibres provide similar service and that raises a key question: i.e., how does the varied stiffness between fibres and solids impact on the packing state and overall behaviour. Figure 22c,d shows how the dilative behaviour of sand changes to contractive strain-softening for the major principal stress axis reorientated to 60° from its initial vertical direction, whereas fibres preserve the dilative response, irrespective of principle stress orientation. However, fibres fail to fully perform under compressive–torsional stress environments.

When introduced to clays, fibres are reported to compromise dilation and promote build-up of excess pore-water pressure under undrained shearing conditions [152]. Failure along distinct slip planes within unreinforced clays changes to a barrelling type of failure in fibre-reinforced soils. For clays, typical content of synthetic fibres is 0.2 to 1 wt.%, while for recycled waste fibres, this ratio is higher at between 1 and 5 wt.%.

Fig. 22 Consolidated-undrained (CU) behaviour of sands and fibre-reinforced sands under cyclic and anisotropic loading conditions (a and b): first and second stress–strain hysteresis loops for two sands, mixed with silt and fibre [35]; (c): HCTS CU results for sand, with and without fibre reinforcement, showing stress–strain curves for p' = 400 kPa, α = 30°, and b = 0.5 and 1.0 (compression and torsion) [68]; (d) HCTS results for sand, with and without fibre reinforcement showing stress–strain curves for p' = 400 kPa, α = 60°, b = 0.5 and 1.0 (torsion). Note: HCTS, hollow cylinder torsional shear; p', effective mean normal stress; α*,* principal stress orientation to vertical direction; b*,* intermediate principal stress ratio [68]

Fibre typology

Figure 23 presents snapshots of a range of common natural and synthetic fibre types employed in ground engineering. These include natural fibres of wool, jute [153], coir [70], sisal, palm, and flax, and synthetic fibres of polypropylene [142], nylon, fibreglass, rubber, polyvinyl alcohol [154], polyethylene and polyamide. Common recycled fibres used in ground improvement are a range of scrap tyre materials spanning across the particle-size range spectrum, including granulated tyre (sizing from 425 µm to 12 mm), tyre chips (sizing from 12 to 50 mm), and tyre shreds (sizing from 50 to 305 mm) [32].

Employment of unconventional upcycled fibres has attracted some recent interest, including shred waste-carpet fibres [155], and precipitated calcium carbonate (PCC) obtained from sucrose ($C_{12}H_{22}O_{11}$) juice purification during sugar production [156].

Fig. 23 Examples of natural, synthetic and recycled fibres sometimes mixed in soil to imitate plant rootlet reinforcement effect: (a) coir [157]; (b) nylon – virgin synthetic [157]; (c) polypropylene – virgin synthetic [157]; (d) fibreglass – virgin synthetic [157]; (e-f) waste carpet [155]; (g) jute [153 – with permission from ASCE]; (h): coir [70]; (i) thermoplastic polymeric microsynthetic [68]; (j) granulated tyre [158]

3.2.2 Imitating weathered minerals

[159] attributed the origin of amorphous silica in soil to chemical and thermal weathering and series of dissolution–reprecipitation processes. Amorphous silica in soil can appear in the form of a smooth 'onionskin' shield around quartz particles, or individual rounded flocs that occupy soil pore spaces [160]. The coating and filling functions of these fine weathered minerals in soil have led to a surge in development of a range of nanomaterials, including nano-silica (NS) and nano-clay (NC). Recent contributions include the use of colloidal NS hydrosols in reconstruction of naturally porous loessic brickearths [25], and to mediate a range of soils, including dune sands [161] and peat [162].

Weathering of minerals can lead to geochemical changes in soil, triggering a range of reactions that can generate novel binders. A simple form of such reactions is deprotonation of clays in alkaline environments, and formation of C-S-H gels in the presence of calcium source. The binding matrix can be imitated to synthesise complex geopolymers. Geopolymerisation refers to thermal and chemical interactions between aluminosilicate-rich materials (e.g., clay, fly ash (FA), slag) and alkaline solutions (e.g., NaOH, Na_2SiO_3) for formation of inorganic polymers of alumina and silica. The process resembles hydration of Portland cement, but leaves behind little carbon footprint. Using geopolymerisation for stabilisation of domestic solid wastes has gained some recent interest; for instance, [163] deployed geopolymerisation to stabilise spent ground coffee (collected from coffee brewing cafes) into road subgrades. Other novel forms of geopolymers used in ground engineering include FA and slag-based geopolymers [164], FA–calcium-carbide residue CCR (by-product of acetylene gas production) based geopolymers [165], recycled asphalt pavement (RAP) and FA geopolymer [166], as well as eggshell powder (from crushing waste eggshells) and FA (from coal-fired electricity production plant) [167].

3.2.3 Engineered biological matters (synthetic biology)

Bone is an adaptive living material. When loaded repeatedly, bone responds to the stimulus and cells grow to make the system stronger. There is interest to engineer simple organisms to have this type of responsive behaviour (i.e., different from how they behave in nature). This idea was the philosophy behind the recent Newcastle University and University of Northumbria 'Thinking Soils' project, which aims to develop a material containing engineered bacteria that strengthens itself in respond to load. The project concept [168] was to create a volume of soil (Fig 24a) that is saturated with water, all the nutrients that bacteria need present, along with bacteria that are engineered to respond to pressure. When load is applied, the porewater pressure in the soil volume rises, and the bacteria respond to that pressure by initiating a process of calcium carbonate cementation. As the load is maintained, pressure is maintained, and the soil becomes strengthened in response. At the laboratory scale, genetically engineered bacteria are grown in agar-based hydrogels (see Fig. 24c for microstructure), which have some similar mechanical properties to clays [169]. In these experiments, the hydrogel acts as a soil analogue, which allows good visualisation of the bacteria and control over culturing and growth in 3D.

Imitation of bones may also attract the interest of the permafrost research. Permafrost is a complex multiphase porous material, comprised of ice lenses, pore ice, unfrozen water and air. Characterisation of permafrost as a porous medium depends on the amount of ice and unfrozen water in the pores, which is nearly impossible to determine through common intrusive and non-intrusive geophysical techniques. Recently, [171] reported on transient acoustic waves propagating in a cancellous bone-like material and the use of theory of poroelasticity to study the effects of porosity and pore fluid on the stress distribution, deformation, and reflected and transmitted pressures of the bone-like material. The idea was extrapolated in [172-173] for non-destructive determination of bulk modulus, shear modulus, porosity, unfrozen water content and ice content of permafrost material.

5. Closing Remarks

It is intuitively established that the geomechanical behaviour of natural soils varies within, and depends on their frame elements, bonding elements, voids that accommodate air, water and microorganisms, and importantly the form and structure that relates these to one another. As such, natural soil behaviour encompasses a wealth of chemo-bio-physical processes. Frame elements vary in size, sorting, shape, texture, and crystalline properties. In natural form, elements and systems that make up natural soils are self-healing, self-producing, and self-forming. They constantly evolve, adopt form and roles in response to environment, and re-establish functions that are disrupted in the natural erosive and stress environment. These *properties*, collectively, mark the fundamental difference between natural and engineered ground, as two different types of grand systems. Engineered ground is a product of mechanical and/or chemical densification, with a sole mission of enhancing stiffness, and stress at steady states, at the cost of filling and compacting void spaces, and replacing air, water and microorganisms therein with calcium-based cements, and alike. This transforms the natural ground into a self-standing (e.g., for cuttings), impermeable (to control groundwater or line buried solid wastes), strong and stiff (to bear superstructure loads) medium. This also disrupts the biogeochemical cycles and self-forming, self-healing capacities of forms and structures, which are reliant on the soils' intertwining pore network, and driven by interaction amongst frame and bonding elements, and also the living organisms.

To this end, and in the context of NiSE, the next generation of engineering interventions should achieve the following objectives: (1) eliminate the need for exogenous contact-point reinforcement by manipulating soil grain surface properties; (2) employ alternative bonding agents that offer greater toughness and ductility than traditional (brittle) materials; (3) form a porous cemented system that accepts bond breaking as an inevitability, but which is capable of adapting and self-repairing through an autonomous response to damage. In this, engineered ground in the context of NiSe is more sustainable (allowed to continue having functions well beyond a source of heat, water, minerals, and stiff foundation), resilient (arranged to continue functioning in the face of extreme climates), self-forming (designed to be reliant on interactions among self-producing, self-healing evolving components), and adaptable, all contributing to enhanced societal wellbeing (refer to Fig. 1a). Through re-establishing the balance between engineered and natural systems in ground, and also restoration of degraded ground function in line with the NiSE concept of appropriating the methods, materials and models according to the above objectives, this paper presented various examples to illustrate how the ground engineering is being rethought, and how ground is being rebalanced with natural systems.

Fig. 24 Sculpting soil responses to force by altering sequences of DNA and through the interaction of many different genetic devices and engineered organisms: (a) artists impression of a bio-based self-constructing foundation [169]; (b) unconfined compression performed on a column of agarose gel [170]; (c) microstructure of Agarose LM gel [169]; (d) simulation of multilateral flow (growth media for bacteria) and implications of 3D architecture of cementation in sands [119]; (e-f) 3D sand forms, scanned as excavation takes place, in seeking an insight into cementation process [119]

6. Conclusions

The ideal engineered ground within the NiSE framework is a complex ground system, in that its constituting geologic and biogenic elements and systems are adaptive, responsive, self-healing, self-producing, self-forming, fractal and intertwined. Instated within is at least one of four basic types of imitable traits abstracted from nature: i.e., forms, materials, generative processes and functions.

Key findings drawn from this contribution are:

1. NiSE is translated into an adaptability indicator system. This is a simple vetting tool, illustrated in Fig. 1b, for bio-inspired/mimetic materials used in ground engineering. Materials receive a five-scoring scale in three categories of forms, functions and processes. Methods and models enable materials to be instated in ground.

2. Models, in the NiSE context, drape a spectrum of scales, from nano- to meso- to micro.

* Nanoscale models avail studying atomistic-level interactions between biomimetic substances and soil particles. These include dissolution, precipitation, nucleation, evolution, ageing, and degradation in a thermodynamics and kinetics context.

* Mesoscale models give insight into rate and mechanisms of nanoparticle agglomeration and self-organisation of minerals and biogenic substances. Techniques lag behind in simulating long timescale processes (e.g., fatigue and hydration) in small length scales.

* Microscale models allow an abstraction of reality through creating contact/rheological models. Findings directly feed into constitutive models and design. When paired with spectroscopic methods (e.g., coupled LSDEM and μCT), the combined technology allows accurate determination of contact force distribution among particles of measured morphology.

* Engineered soils, in the NiSE context, demand bespoke or adjusted constitutive models. There is scope for further development of mesoscale models to incorporate complex long-timescale processes, like fragmentation and particle breakage, and ways the bio-inspired/mediated materials intervene, into future constitutive models. Coupled microscale models with imaging techniques can similarly be of benefit. A recent technological solution is making combined use of DEM (an established microscale technique), in-situ synchrotron radiography, and thermographic imaging.

* Engineering structured and fissured fine soils, particularly when mixed with bio-inspired fibrous matters, could largely benefit from advances in microscale models as standalone, or in conjunction with imaging techniques (particularly CT).

3. Methods for visualisation of particle-level events have seen substantial recent advances.

* µCT inform micro-scale models through visualising the size, shape, topology, and evolution of pore throats, interacting rigid and soft particles, and fines movement through pore networks.

* PIV uses consecutive imaging of individual particles in movement within a particulate media. There is scope for wider use of PIV in studying the inherent and induced anisotropy in engineered soils.

* CT provides real-time images of soil pore spaces in evolution, also evolving orientation and tortuosity of fibrous matters in soil.

4. Advances and new avenues of research on bio-mediated materials are summarised here;

* Deep rooted C3- and C4-cycle crops benefit in relaxing and curbing temperature fluctuations in the subsoil. Key gains are enhanced levels of saturated hydraulic conductivity, lowered air-entry value and adjusted water retention capacity to levels typical for coarser soils. A key obstacle, however, is the time required for the growth of plants. When used in conjunction with viscose biopolymer solutions, mechanical benefits materialise from the outset, and growth of rootlets gain momentum in the presence of excess carbon, nitrogen and nutrients.

* Over 15 types of biocements, with varying constituting salt structure, biopolymer, pH-controlling and bio-controlling components, are established with scopes as pore void infill or soil biocrust; yet, the cost revolves typically around 2 to 2.5-times greater compared to that for Portland cement.

* Bacterial biofilms, products of bacteria multiplication on surfaces, form as soft, viscous, ductile and elastomeric binders in soil pores, in between and around soil particles, and pore throats. They benefit in enhanced damping and small-strain stiffness, but risk modest decrease in permeability and a potential of resonance under high-frequency cyclic loads. Research is tending towards development of biofilms that offer a decrease in P- and S-wave peak-to-peak amplitudes and faster wave attenuation.

* Biological CPT, via ureolysis and EICP (where enzymes are from agricultural sources), can benefit in a number of ways, including strength improvement of sands, capture of trace metals and radionuclides, at a cost of modest decrease in void ratio. However, large-scale trials have largely failed to attract interest due to cost, logistical constraints, and possible implications of toxic ammonium chloride from ureolysis.

* MIDP is an emerging safer and cheaper alternative to CPT and EICP. The technique involves stimulation of indigenous microbes to produce non-hazardous biogas and biominerals.

* Microbial CPT (MICP) is relatively better established and enjoys a body of published articles on full scale (field) testing. Loss of permeability through biomass clogging continues to be a concern.

* Biostimulation of native microbes, as an MICP technique, is receiving increasing interest. Eutrophication remains an environmental constraint, as the technique requires biomass enriching through addition of organic nutrients, such as molasses.

* Biopolymers offer better ductility, lower cost, rapid treatment, and an opportunity for quality control post-application. However, their application to ground may lead to heating, change in soil pH, and pore clogging.

5. Advances and new avenues of research on bio-inspired materials are summarised here;

* Future research on the development of genetically engineered bacteria that exhibit pressure-responsive behaviour shows promise; as does the use of bacterial spores entombed in grouts that germinate upon exposure to air, thereby assisting damaged binders to self-heal; and the utilisation of fungal networks to create water-repellent hydrophobic surfaces as a means for erosion control.

* Future sees research into unconventional, upcycled fibres types, and ways for their appropriate and optimum uses in strengthening soils with high fines content.

* Recent attempts in imitation of natural weathering of minerals has led to a surge in development of NS, NC, and inorganic geopolymers of alumina and silica, with very little carbon footprint. This is a novel branch of research, with emphasis on geopolymerisation, that allows the use of unconventional wastes (e.g., sugar refinery wastes, spent ground coffee, and eggshell) in ground improvement.

Acknowledgements

This contribution partly reports the outcomes of the first NiSE Workshop (NiSE1) that took place online (hosted from London, UK) 11–12th February 2021. The workshop organisers thank Prof Catherine O'Sullivan and Prof Hassan Abdalla for opening the sessions. They also thank Prof Volodymyr Ivanov, Dr Victor Stabnikov, Dr Gil H. Ochoa Gonzalez, Dr Jose Manuel Ramirez Leon, Prof Liz Varga, Prof Darryl Newport, Dr Bamdad Ayati, Dr Bilal Kaddouh, Dr Mehran Eskandari Torbaghan, Dr Munsamy Logan, Dr Sohrab Donyavi, and Dr Aryan Hojjati for their contributions to the workshop. .

References

[1] Assadi-Langroudi A, Jefferson I, O'Hara-Dhand K, Smalley I (2014) Micromechanics of quartz sand breakage in a fractal context. Geomorphology, 211:1-10

[2] Assadi Langroudi A, Theron E (2019) Gaps in particulate matters: Formation, mechanisms, implications. In Jacobsz SW (Ed) Proceedings of the 17th African Regional Conference on Soil Mechanics and Geotechnical Engineering, International Society for Soil Mechanics and Geotechnical Engineering, pp 169-179.

[3] ISO 18458 (2015) Biomimetics – Terminology, concepts and methodology. International Organization for Standards, Geneva, Switzerland.

[4] Vincent JFV (2009) Biomimetics - A review. Proceedings of the Institution of Mechanical Engineers, Part H: Journal of Engineering in Medicine, 223(8):919-939.

[5] Gruber P, Bruckner D, Hellmich C, Schmiedmayer HB, Stachelberger H, Gebeshuber IC (2011) Biomimetics - Materials, Structures and Processes: Examples, Ideas and Case Studies. Springer-Verlag Berlin Heidelberg.

[6] Aristotle (2008) Aristotle Physics. In Bostock D (Ed), Waterfield R (Translator). OUP Oxford, pp 38-41

[7] Assadi-Langroudi A, Theron E, Ghadr S (2021) Sequestration of carbon in pedogenic carbonates and silicates from construction and demolition wastes. Construction and Building Materials, 286: 122658

[8] Masoero E (2021) Simulating the chemo-mechanical behaviour of minerals at the nano-to-micro mesoscale, In First NiSE Workshop (NiSE1), 11-12 February, University of East London, London, UK.

[9] Ebrahimi D, Pellenq RJM, Whittle AJ (2016) Mesoscale simulation of clay aggregate formation and mechanical properties. Granular Matter, 18(3):1-8.

[10] Bandera S, O'Sullivan C, Angioletti-Uberti S, Tangney P (2019) An evaluation of contact models for particle-scale simulation of clay. E3S Web of Conferences, EDP Sciences, 92:14001.

[11] Hanley KJ, O'Sullivan C, Byrne EP, Cronin K (2012) Discrete element modelling of the quasi-static uniaxial compression of individual infant formula agglomerates. Particuology, 10(5):523-531.

[12] Su TC, O'Sullivan C, Nagira T, Yasuda H, Gourlay CM (2019) Semi-solid deformation of Al-Cu alloys: A quantitative comparison between real-time imaging and coupled LBM-DEM simulations. Acta Materialia, 163:208-225.

[13] Altuhafi FN, O'Sullivan C, Sammonds P, Su TC, Gourlay CM (2021) Triaxial compression on semi-solid alloys. Metallurgical and Materials Transactions A, 52(5):2010-2023.

[14] O'Sullivan C (2021) How can fundamental modelling and observation inform NISE? In First NiSE Workshop (NiSE1), 11-12 February, University of East London, London, UK.

[15] Mesinc (2021) Metrics engineering supply chains. https://www.mesinc.net/. Accessed 09 July 2021.

[16] Fathalikhani M, Graham J, Kurz D, Maghoul P (In Press) Investigation and modification of a CSSM-based elastic–thermoviscoplastic model for clay, International Journal of Geomechanics (ASCE).

[17] Safavizadeh S, Montoya BM, Gabr MA (2019) Microbial induced calcium carbonate precipitation in coal ash. Géotechnique, 69(8): 727-740.

[18] Hall SA, Bornert M, Desrues J, Pannier Y, Lenoir N, Viggiani G, Bésuelle P (2010) Discrete and continuum analysis of localised deformation in sand using X-ray μCT and volumetric digital image correlation. Géotechnique, 60(5): 315-322.

[19] Andò E, Hall SA, Viggiani G, Desrues J, Bésuelle P (2012a) Experimental micromechanics: Grain-scale observation of sand deformation. Géotechnique Letters, 2(3):107-112.

[20] Andò E, Hall SA, Viggiani G, Desrues J, Bésuelle P (2012b) Grain-scale experimental investigation of localised deformation in sand: A discrete particle tracking approach. Acta Geotechnica 7(1):1-13.

[21] Cygan RT, Kubicki JD (2001) Molecular modeling theory: Applications in the geosciences, De Gruyter, https://doi.org/10.1515/9781501508721.

[22] Duque Redondo E (2018) Atomistic simulations of confined species in 2D nanostructures: clays and CSH gel. PhD Dissertation, University of the Basque Country, Spain.

[23] Buchy HN, Katti KS, Katti DR (2020) Modeling the behavior of organic kerogen in the proximity of calcite mineral by molecular dynamics simulations, Energy and Fuels, 34(3):2849-2860.

[24] Gu W, Li X, Li Q, Hou Y, Zheng M, Li Y (2021) Combined remediation of polychlorinated naphthalene-contaminated soil under multiple scenarios: An integrated method of genetic engineering and environmental remediation technology. Journal of Hazardous Materials, 405: 124139.

[25] Assadi-Langroudi A (2014) Micromechanics of Collapse in Loess. PhD Dissertation, University of the Birmingham, England, UK.

[26] Bauchy M, Masoero E, Ulm FJ, Pellenq R (2015) Creep of bulk CSH: insights from molecular dynamics simulations. CONCREEP 10:511-516.

[27] Shvab I, Brochard L, Manzano H, Masoero E (2017) Precipitation mechanisms of mesoporous nanoparticle aggregates: off-lattice, coarse-grained, kinetic simulations. Crystal Growth and Design, 17(3):1316-1327.

[28] Ofiteru ID, Masoero E, Taniguchi D, Gebhard S, Mihai I, Jefferson T, Paine K (2020) Engineering microbial-induced carbonate precipitation via meso-scale simulations. ASCE Engineering Mechanics Institute International Conference, Durham University, Durham, England, UK.

[29] Coopamootoo K, Masoero E (2020) Simulations of crystal dissolution using interacting particles: Prediction of stress evolution and rates at defects and application to tricalcium silicate. Journal of Physical Chemistry C, 124(36):19603-19615.

[30] Huang X, Hanley KJ, O'Sullivan C, Kwok FC (2014) Effect of sample size on the response of DEM samples with a realistic grading. Particuology, 15:107-115.

[31] Assadi-Langroudi A, Jefferson I (2013) Collapsibility in calcareous clayey loess: A factor of stress-hydraulic history. Int J Geomate Geotech Constr Mater Environ, 5(1):620-626

[32] Ghadr S, Samadzadeh A, Bahadori H, O’Kelly BC, Assadi-Langroudi A (2021) Liquefaction resistance of silty sand with ground rubber additive. International Journal of Geomechanics, 21(6):04021076. https://doi.org/10.1061/(ASCE)GM.1943-5622.0002002

[33] Assadi-Langroudi A, Jefferson I (2016) The response of reworked aerosols to climate through estimation of inter-particle forces. International Journal of Environmental Science and Technology, 13(4):1159-1168.

[34] McDougall J, Kelly D, Barreto D (2013) Particle loss and volume change on dissolution: Experimental results and analysis of particle size and amount effects. Acta Geotech, 8:619–62.

[35] Ghadr S, Samadzadeh A, Bahadori H, Assadi-Langroudi A (2020) Liquefaction resistance of fibre-reinforced silty sands under cyclic loading. Geotextiles and Geomembranes, 48(6):812-827

[36] Shire T, O’Sullivan C, Taylor H, Sim WW (2014) Measurement of constriction size distributions using three grain-scale methods. Proceedings of the 8th International Conference on Scour and Erosion, Oxford, UK, CRC Press

[37] Garcia FE, Bray JD (2018a) Distinct element simulations of shear rupture in dilatant granular media. International Journal of Geomechanics, 18(9):04018111

[38] Garcia FE, Bray JD (2018b) Distinct element simulations of earthquake fault rupture through materials of varying density. Soils and Foundations, 58(4):986-1000

[39] Hazeghian M, Soroush A (2015) DEM simulation of reverse faulting through sands with the aid of GPU computing. Computers and Geotechnics, 66:253-263.

[40] Garcia FE, Bray JD (2019a) Discrete element analysis of earthquake fault rupture-soil-foundation interaction. Journal of Geotechnical and Geoenvironmental Engineering, 145(9):04019046

[41] Garcia FE, Bray JD (2019b) Discrete-element analysis of influence of granular soil density on earthquake surface fault rupture interaction with rigid foundations. Journal of Geotechnical and Geoenvironmental Engineering, 145(11): 04019093.

[42] Kawamoto R, Andò E, Viggiani G, Andrade JE (2016) Level set discrete element method for three-dimensional computations with triaxial case study. Journal of the Mechanics and Physics of Solids, 91:1-13

[43] Kawamoto R, Andò E, Viggiani G, Andrade JE (2018) All you need is shape: Predicting shear banding in sand with LS-DEM. Journal of the Mechanics and Physics of Solids, 111:375-392

[44] Harmon JM, Karapiperis K, Li L, Moreland S, Andrade JE (2021) Modeling connected granular media: Particle bonding within the level set discrete element method. Computer Methods in Applied Mechanics and Engineering, 373:113486.

[45] Ghadr S, Fatehfar N, Bahadori H, Assadi-Langroudi A (2021) Static flow and post failure sediment yield in loose silty sands. Journal of Geotechnical and Geoenvironmental Engineering (in press).

[46] Silva Dos Santos AP, Consoli NC, Baudet BA (2010) The mechanics of fibre-reinforced sand. Géotechnique, 60(10):791–799.

[47] Li M, He H, Senetakis K (2017) Behavior of carbon fiber-reinforced recycled concrete aggregate. Geosynthetics International, 24(5):480-490.

[48] Fu R, Baudet BA, Madhusudhan BN, Coop MR (2018) A comparison of the performances of polypropylene and rubber fibers in completely decomposed granite. Geotextiles and Geomembranes, 46(1):22-28.

[49] Madhusudhan BN, Baudet BA, Ferreira PMV, Sammonds P (2017) Performance of fiber reinforcement in completely decomposed granite. Journal of Geotechnical and Geoenvironmental Engineering, 143(8): 1-11.

[50] Ekinci A (2019) Effect of preparation methods on strength and microstructural properties of cemented marine clay. Construction and Building Materials, 227:116690.

[51] Hight DW, Ellison RA, Page DP (2004) Engineering in the Lambeth Group London: Ciria.

[52] Hight DW, Gasparre A, Nishimura S, Minh NA, Jardine RJ, Coop MR (2007) Characteristics of the London clay from the Terminal 5 site at Heathrow Airport. Géotechnique, 57(1):3–18.

[53] Skempton AW, Petley DJ (1967) The strength along structural discontinuities in stiff clays. In Proceedings of the Geotechnical Conference Oslo, Norway: pp 29–45.

[54] Marsland A (1971) The shear strength of stiff fissured clays. In Proceedings of the Roscoe Memorial Symposium Cambridge, UK: 59–68.

[55] Gasparre A, Hight DW, Nishimura S, Minh NA, Jardine RJ, Coop MR (2007) The influence of structure on the behaviour of London Clay. Géotechnique, 57(1):19–31

[56] Vitone C, Cotecchia F (2011) The influence of intense fissuring on the mechanical behaviour of clays. Géotechnique, 61(12):1003–1018.

[57] Fearon RE, Coop MR (2002) The influence of landsliding on the behaviour of a structurally complex clay. Quarterly Journal of Engineering Geology and Hydrogeology, 35(1):25–32.

[58] Fonseca J (2011) The evolution of morphology and fabric of a sand during shearing. Dissertation, Imperial College London, London, England, UK.

[59] Shire T, O'Sullivan C (2016) Constriction size distributions of granular filters: A numerical study. Géotechnique, 66(10):826-839.

[60] Shire T, O'Sullivan C (2017) A network model to assess base-filter combinations. Computers and Geotechnics, 84:117-128.

[61] Kenney TC, Chahal R, Chiu E, Ofoegbu GI, Omange GN, Ume CA (1985) Controlling constriction sizes of granular filters. Canadian Geotechnical Journal, 22(1):32-43.

[62] Anselmucci F, Andó E, Sibille L, Lenoir N, Peyroux R, Arson C, Bengough AG (2019) Root-reinforced sand: Kinematic response of the soil. In Proceedings of the 7th International Symposium on Deformation Characteristics of Geomaterials, IS-Glasgow, EDP Sciences, pp 12011

[63] Kim SY, Park J, Cha W, Lee JS, Carlos Santamarina, J (2021) Soil response during globally drained and undrained freeze–thaw cycles under deviatoric loading. Journal of Geotechnical and Geoenvironmental Engineering, 147(2):06020030.

[64] Fonseca J, Riaz A, Bernal-Sanchez J, Barreto D, McDougall J, Miranda-Manzanares M, Marinelli A, Dimitriadi V (2019) Particle-scale interactions and energy dissipation mechanisms in sand–rubber mixtures. Géotechnique Letters, 9(4):263-268

[65] Stamati O, Andò E, Roubin E, Cailletaud R, Wiebicke M, Pinzon G, Birmpilis G (2020) spam: Software for Practical Analysis of Materials. Journal of Open Source Software, 5(51):2286.

[66] Mirzababaei M, Mohamed M, Miraftab M (2017) Analysis of strip footings on fiber-reinforced slopes with the aid of particle image velocimetry. Journal of Materials in Civil Engineering, 29(4):04016243.

[67] Wang Y, Hu Y, Hossain MS (2020) Soil flow mechanisms of full-flow penetrometers in layered clays through particle image velocimetry analysis in centrifuge test. Canadian Geotechnical Journal, 57(11):1719-1732.

[68] Ghadr S, Bahadori H, Assadi-Langroudi A (2019) Anisotropy in sand–fibre composites and undrained stress–strain implications. International Journal of Geosynthetics and Ground Engineering, 5(3):1-13.

[69] Mandolini A, Diambra A and Ibraim E (2019) Strength anisotropy of fibre-reinforced sands under multiaxial loading. Géotechnique, 69(3):203-216.

[70] Mirzababaei M, Anggraini V, Haque A (2020) X-ray computed tomography imaging of fibre-reinforced clay subjected to triaxial loading. Geosynthetics International, 27(6):635-645.

[71] Kavazanjian E, van Paassen L (2019) Biogeotechnical mitigation of earthquake-induced soil liquefaction. NHERI Workshop, Portland, Oregon, USA.

[72] Tang AM, Hughes PN, Dijkstra TA, Askarinejad A, Brenčič M, Cui YJ, Diez JJ, Firgi T, Gajewska B, Gentile F, Grossi G, et al. (2018) Atmosphere–vegetation–soil interactions in a climate change context; Impact of changing conditions on engineered transport infrastructure slopes in Europe. Quarterly Journal of Engineering Geology and Hydrogeology, 51(2):156-168

[73] Yu Z, Eminue OO, Stirling R, Davie C, Glendinning S (2021) Desiccation cracking at field scale on a vegetated infrastructure embankment. Géotechnique Letters, 11(1):88-95.

[74] Emadi-Tafti M, Ataie-Ashtiani B (2019) A modeling platform for landslide stability: A hydrological approach. Water, 11(10):2146.

[75] Tagarelli V (2019) Analysis of the Slope-Vegetation-Atmosphere Interaction for the Design of the Mitigation Measures of Landslide Risk in Clayey Slopes. PhD Dissertation, Politecnico di Bari, Bari, Italy.

[76] Cotecchia F, Tagarelli V, Pedone G, Ruggieri G, Guglielmi S, Santaloia F (2019) Analysis of climate-driven processes in clayey slopes for early warning system design. Proceedings of the Institution of Civil Engineers - Geotechnical Engineering, 172(6):465-480.

[77] Cotecchia F, Pedone G, Bottiglieri O, Santaloia F, Vitone C (2014) Slope-atmosphere interaction in a tectonized clayey slope: A case study. Italian Geotechnical Journal, 1(14):34-61.

[78] Evans JR (1989) Photosynthesis and nitrogen relationships in leaves of C3 plants. Oecologia 78:9-19.

[79] Flexas J, Medrano H (2002) Drought-inhibition of photosynthesis in C3 plants: stomatal and non-stomatal limitations revisited. Ann. Bot., 89:183-189.

[80] Ghannoum O (2009) C4 photosynthesis and water stress. Ann Bot., 103(4):635-44. doi: 10.1093/aob/mcn093.

[81] Christin PA, Osborne CP (2014) The evolutionary ecology of C4 plants. New Phytologist, 204(4):765–781. doi:10.1111/nph.13033.

[82] Hogan CM (2011) Respiration. Encyclopaedia of Earth. In McGinley M, Cleveland CJ (Ed). National Council for Science and the Environment. Washington, D.C.

[83] Sage RF, Sage TL, Kocacinar F (2012) Photorespiration and the evolution of C4 photosynthesis. Annual Review of Plant Biology, 63(1):19–47. doi:10.1146/annurev-arplant-042811-105511.

[84] Neris J, Jiménez C, Fuentes J, Morillas G, Tejedor M (2012) Vegetation and land-use effects on soil properties and water infiltration of Andisols in Tenerife (Canary Islands, Spain). CATENA, 98:55-62.

[85] Wang C, Zhao C, Xu Z, et al. (2013) Effect of vegetation on soil water retention and storage in a semi-arid alpine forest catchment. J. Arid Land, 5:207-219. https://doi.org/10.1007/s40333-013-0151-5

[86] Leung AK, Garg A, Ng CWW (2015) Effects of plant roots on soil-water retention and induced suction in vegetated soil. Eng Geo, 193:183–197. doi:10.1016/j.enggeo.2015.04.017

[87] Tagarelli (2021) Preliminary field data of selected deep-rooted vegetation effects on the slope-vegetation-atmosphere interaction: Results from an in-situ test. In First NiSE Workshop (NiSE1), 11-12 February, University of East London, London, UK.

[88] Ivanov V, Stabnikov V (2016) Construction Biotechnology: Biogeochemistry, Microbiology and Biotechnology of Construction Materials and Processes. Springer.

[89] Hatch H (2020) Bryce Canyon City, UT, USA. https://unsplash.com/photos/QJ0rRpumcVM Accessed 09 July 2021.

[90] Leonardi S (2020) Arches National Park, Utah, USA. https://unsplash.com/photos/1UWJt8glpt8 Accessed 09 July 2021.

[91] Sahatchiev H (2019) Belogradchik, Vidin, Bulgaria. https://unsplash.com/photos/iQS2BCfHc10 Accessed 09 July 2021.

[92] Ivanov V (2011) Environmental Microbiology for Engineers. CRC press.

[93] Ivanov V, Stabnikov V, Kawasaki S (2019) Ecofriendly calcium phosphate and calcium bicarbonate biogrouts. Journal of Cleaner Production, 218:328-334.

[94] Berlanga M, Guerrero R (2016) Living together in biofilms: The microbial cell factory and its biotechnological implications. Microbial Cell Factories, 15(1):1-11

[95] Ta HX (2016) Microbial biofilm in porous sediments: Effects on soil behaviour. PhD Dissertation, Washington State University, USA

[96] Ta HX, Muhunthan B, Ramezanian S, Abu-Lail N, Kwon TH (2017) Effects of bacterial dextran on soil geophysical properties. Environmental Geotechnics, 5(2):114-122

[97] Fujita Y, Taylor JL, Wendt LM, Reed DW, Smith RW (2010) Evaluating the potential of native ureolytic microbes to remediate a 90Sr contaminated environment. Environmental Science and Technology, 44(19):7652-7658

[98] Ghosh S, Biswas M, Chattopadhyay BD, Mandal S (2009) Microbial activity on the microstructure of bacteria modified mortar. Cement and Concrete Composites, 31(2):93-98

[99] Cunningham AB, Gerlach R, Spangler L, Mitchell AC (2009) Microbially enhanced geologic containment of sequestered supercritical CO_2. Energy Procedia, 1(1):3245-3252

[100] Tobler DJ, Cuthbert MO, Greswell RB, Riley MS, Renshaw JC, Handley-Sidhu S, Phoenix VR (2011) Comparison of rates of ureolysis between *Sporosarcina pasteurii* and an indigenous groundwater community under conditions required to precipitate large volumes of calcite. Geochimica et Cosmochimica Acta, 75(11):3290-3301

[101] Krishnan V, Khodadadi Tirkolaei H, Martin K, Hamdan N, van Paassen LA, Kavazanjian Jr E (2021) Variability in the unconfined compressive strength of EICP-treated “standard” sand. Journal of Geotechnical and Geoenvironmental Engineering, 147(4): 06021001

[102] van Paassen (2021) Centre for bio-mediated and bio-inspired geotechnics. In First NiSE Workshop (NiSE1), 11-12 February, University of East London, London, UK.

[103] Ivanov V, Stabnikov V, Stabnikova O, Kawasaki S (2019) Environmental safety and biosafety in construction biotechnology. World Journal of Microbiology and Biotechnology, 35(2):26

[104] Abbasi B, Ta HX, Muhunthan B, Ramezanian S, Abu-Lail N, Kwon TH (2018) Modeling of permeability reduction in bioclogged porous sediments. Journal of Geotechnical and Geoenvironmental Engineering, 144(4):06018016

[105] El Mountassir, G, Minto JM, van Paassen LA, Salifu E, Lunn RJ (2018) Applications of microbial processes in geotechnical engineering. Advances in Applied Microbiology, 104:39-91

[106] van Paassen LA (2009) Biogrout, Ground Improvement by Microbial Induced Carbonate Precipitation. PhD dissertation, TU Delft, The Netherlands

[107] van Paassen LA, van Loosdrecht MCM, Pieron M, Mulder A, Ngan-Tillard DJM, van der Linden TJM (2010) Strength and deformation of biologically cemented sandstone, In Vrkljan (ed), I Rock Engineering in Difficult Ground Conditions – Soft Rocks and Karst, pp 405-410

[108] van Paassen LA, Ghose R, van der Linden TJ, van der Star WR, van Loosdrecht MC (2010) Quantifying biomediated ground improvement by ureolysis: Large-scale biogrout experiment. Journal of Geotechnical and Geoenvironmental Engineering, 136(12):1721-1728

[109] Minto JM, Hingerl FF, Benson SM, Lunn RJ (2017) X-ray CT and multiphase flow characterization of a 'bio-grouted' sandstone core: The effect of dissolution on seal longevity. International Journal of Greenhouse Gas Control, 64:152-162

[110] Burbank MB, Weaver TJ, Williams BC, Crawford RL (2012) Urease activity of ureolytic bacteria isolated from six soils in which calcite was precipitated by indigenous bacteria. Geomicrobiology, 29(4):389-395

[111] Svirčev Z, Marković SB, Stevens T, Codd GA, Smalley I, Simeunović J, Obreht I, Dulić T, Pantelić D, Hambach U (2013) Importance of biological loess crusts for loess formation in semi-arid environments. Quaternary International, 296:206-215.

[112] De Jong JT, Soga KS, Kavazanjian E, Burns S, van Paassen LA, Al Quabany A, Aydilek A, Bang SS, Burbank M, Caslake LF, Chen CY, Cheng X, Chu J, Ciurli S, Esnault-Filet A, Fauriel S, Hamdan N, Hata T, Inagaki Y, Jefferis S, Kuo M, Laloui L, Larrahondo J, Manning DAC, Martinez B, Montoya BM, Nelson DC, Palomino A, Renforth P, Santamarina JC, Seagren EA, Tanyu B, Tsesarsky M, Weaver T (2013)

Biogeochemical processes and geotechnical applications: Progress, opportunities and challenges. Géotechnique, 63(4):287-301

[113] Shahrokhi-Shahraki R, Zomorodian SMA, Niazi A, O'Kelly BC (2015) Improving sand with microbial-induced carbonate precipitation. Proceedings of the Institution of Civil Engineers-Ground Improvement, 168(3):217-230. https://doi.org/10.1680/grim.14.00001

[114] Amin M, Zomorodian SMA, O'Kelly BC (2017) Reducing the hydraulic erosion of sand using microbial-induced carbonate precipitation. Proceedings of the Institution of Civil Engineers-Ground Improvement, 170(2):112-122. https://doi.org/10.1680/jgrim.16.00028

[115] Zomorodian SMA, Ghaffari H, O'Kelly BC (2019) Stabilisation of crustal sand layer using biocementation technique for wind erosion control. Aeolian Research, 40:34-41. https://doi.org/10.1016/j.aeolia.2019.06.001

[116] Haouzi FZ, Courcelles B (2018) Major applications of MICP sand treatment at multi-scale levels: A review. In Proceedings of GeoEdmonton 2018: The 71st Canadian Geotechnical Conference and The 13th Joint CGS/IAH-CNC Groundwater Conference.

[117] Esnault-Filet A, Mosser JF, Monleau S, Sapin L, Gutjahr I (2015) Prix de l'Innovation Solscope: Biocalcis. Public technical report: https://www.solscope.fr/medias/MEMOIRE-TECHNIQUE-Biocalcis-Version-publique-.pdf

[118] Guyet A, Dade-Robertson M, Wipat A, Casement J, Smith W, Mitrani H, Zhang M (2018) Mild hydrostatic pressure triggers oxidative responses in *Escherichia coli.* PloS One, 13(7), pe0200660

[119] Arnardottir TH, Dade-Robertson M, Mitrani H, Zhang M, Christgen B (2021), Turbulent Casting: Bacterial Expression in Mineralized Structures. In ACADIA Association for Computer Aided Design in Architecture

[120] Handley-Sidhu S, Sham E, Cuthbert MO, Nougarol S, Mantle M, Johns ML, Macaskie LE, Renshaw JC (2013) Kinetics of urease mediated calcite precipitation and permeability reduction of porous media evidenced by magnetic resonance imaging. International Journal of Environmental Science and Technology, 10(5):881-890

[121] Kavazanjian E, Hamdan N (2015) Enzyme induced carbonate precipitation (EICP) columns for ground improvement. In IFCEE 2015, pp 2252-2261

[122] Martin KK, Khodadadi TH, Kavazanjian Jr, E (2020) Enzyme-induced carbonate precipitation: Scale-up of bio-cemented soil columns. In Geo-Congress 2020: Biogeotechnics, Reston, VA: ASCE, pp 96-103.

[123] Wang L, van Paassen L, Gao Y, He J, Gao Y, Kim D (2020) Laboratory tests on mitigation of soil liquefaction using microbial induced desaturation and precipitation. Geotechnical Testing Journal, 44(2):520-534

[124] O'Donnell ST, Rittmann BE, Kavazanjian Jr E (2017) MIDP: Liquefaction mitigation via microbial denitrification as a two-stage process I: Desaturation. Journal of Geotechnical and Geoenvironmental Engineering, 143(12):04017094

[125] Tan L, Reeksting B, Ferrandiz-Mas V, Heath A, Gebhard S, Paine K (2020) Effect of carbonation on bacteria-based self-healing of cementitious composites. Construction and Building Materials, 257:119501

[126] Litina C, Al-Tabbaa A (2020) First generation microcapsule-based self-healing cementitious construction repair materials. Construction and Building Materials, 255:119389

[127] Botusharova S, Gardner D, Harbottle M (2020) Augmenting microbially induced carbonate precipitation of soil with the capability to self-heal. Journal of Geotechnical and Geoenvironmental Engineering, 146(4):04020010

[128] Khosravifar A, Moug D (2019) Liquefaction mitigation in silts using microbially induced desaturation. Portland State University

[129] Chen C, Wu L, Harbottle M (2020) Exploring the effect of biopolymers in near-surface soils using xanthan gum–modified sand under shear. Canadian Geotechnical Journal, 57(8):1109-1118

[130] Chang I, Lee M, Tran ATP, Lee S, Kwon YM, Im J, Cho GC (2020) Review on biopolymer-based soil treatment (BPST) technology in geotechnical engineering practices. Transportation Geotechnics, 24:100385.

[131] Khatami HR, O'Kelly BC (2013) Improving mechanical properties of sand using biopolymers. Journal of Geotechnical and Geoenvironmental Engineering, 139(8):1402-1406. https://doi.org/10.1061/(ASCE)GT.1943-5606.0000861

[132] Ni J, Li SS, Ma L, Geng, XY (2020) Performance of soils enhanced with eco-friendly biopolymers in unconfined compression strength tests and fatigue loading tests. Construction and Building Materials, 263:120039

[133] Chang I, Im J, Cho GC (2016) Geotechnical engineering behaviors of gellan gum biopolymer treated sand. Canadian Geotechnical Journal, 53(10):1658-1670

[134] Khatami HR, O'Kelly BC (2018) Prevention of bleeding of particulate grouts using biopolymers. Construction and Building Materials, 192:202-209. https://doi.org/10.1016/j.conbuildmat.2018.10.131

[135] Geng X (2021) Eco-friendly ground improvement techniques for transport infrastructure earthwork. In First NiSE Workshop (NiSE1), 11-12 February, University of East London, London, UK.

[136] Tarantino A, El Mountassir G, Wheeler S, Gallipoli D, Russo G, Augarde C, Urciuoli G, Pirone M, Stokes A, van de Kuilen JW, Gard W (2020) TERRE project: Interplay between unsaturated soil mechanics and low-carbon geotechnical engineering

[137] Salifu E, El Mountassir G (2020) Fungal-induced water repellency in sand. Géotechnique, 71(7):608-615.

[138] Fraccica A, Romero Morales EE, Fourcaud T (2019) Multi-scale effects on the hydraulic behaviour of a root-permeated and compacted soil. IS-Glasgow 2019–7th International Symposium on Deformation Characteristics of Geomaterials, EDP Sciences, pp 1-5.

[139] Salifu E (2019) Engineering Fungal-Mycelia for Soil Improvement. PhD Dissertation, Università degli Studi di Napoli Federico II

[140] Milodowski AE, Northmore KJ, Kemp SJ et al. (2015) The mineralogy and fabric of 'Brickearths' in Kent, UK and their relationship to engineering behaviour. Bull Eng Geol Environ, 74:1187–1211. https://doi.org/10.1007/s10064-014-0694-5

[141] Jamsawang P, Suansomjeen T, Sukontasukkul P, Jongpradist P, Bergado DT (2018) Comparative flexural performance of compacted cement-fiber-sand. Geotextiles and Geomembranes, 46(4):414-425. doi: 101016/jgeotexmem201803008

[142] Tang C, Shi B, Gao W, Chen F, Cai Y (2007) Strength and mechanical behavior of short polypropylene fiber reinforced and cement stabilized clayey soil. Geotextiles and Geomembranes, 25(3): 194–202 doi: 101016/jgeotexmem200611002

[143] Botero E, Ossa A, Sherwell G, Ovando-Shelley E (2015) Stress-strain behavior of a silty soil reinforced with polyethylene terephthalate (PET). Geotextiles and Geomembranes, 43(4):363-369 doi: 101016/jgeotexmem201504003

[144] Yi XW, Ma GW, Fourie A (2015) Compressive behaviour of fibre-reinforced cemented paste backfill. Geotextiles and Geomembranes, 43(3):207-215 doi: 101016/jgeotexmem201503003.

[145] Özkul ZH, Baykal G (2007) Shear behavior of compacted rubber fiber-clay composite in drained and undrained loading. Journal of Geotechnical and Geoenvironmental Engineering, 133(7): 767–781 doi: 101061/(ASCE)1090-0241(2007)133:7(767)

[146] Mirzababaei M, Arulrajah A, Horpibulsuk S, Aldava M (2017) Shear strength of a fibre-reinforced clay at large shear displacement when subjected to different stress histories. Geotextiles and Geomembranes, 45(5):422-429

[147] Tang CS, Li J, Wang DY, Shi B (2016) Investigation on the interfacial mechanical behavior of wave-shaped fiber reinforced soil by pullout test. Geotextiles and Geomembranes, 44(6):872-883 doi: 101016/jgeotexmem201605001

[148] Ayeldeen M, Kitazume M (2017) Using fiber and liquid polymer to improve the behaviour of cement-stabilized soft clay. Geotextiles and Geomembranes, 45(6):592-602 doi: 101016/jgeotexmem201705005

[149] Li Y, Mai YW, Ye L (2005) Effects of fibre surface treatment on fracture-mechanical properties of sisal-fibre composites. Composite Interfaces, 12(1-2):141-163 doi: 101163/1568554053542151

[150] Li C, Zornberg JG (2019) Shear strength behavior of soils reinforced with weak fibers. Journal of Geotechnical and Geoenvironmental Engineering, 145(9):2-8 doi: 101061/(ASCE)GT1943-56060002109

[151] Li C, Zornberg JG (2013) Mobilization of reinforcement forces in fiber-reinforced soil. Journal of Geotechnical and Geoenvironmental Engineering, 139(1):107-115 doi: 101061/(ASCE)GT1943-56060000745

[152] Ekinci A, Ferreira PMV (2012) The undrained mechanical behaviour of a fibre-reinforced heavily over-consolidated clay. ISSMGE - TC 211 International Symposium on Ground Improvement, Brussels, Belgium.

[153] Wang YX, Guo PP, Ren WX, Yuan BX, Yuan HP, Zhao YL, Shan SB, Cao P (2017) Laboratory investigation on strength characteristics of expansive soil treated with jute fiber reinforcement. International Journal of Geomechanics, 17(11):04017101

[154] Mirzababaei M, Arulrajah A, Horpibulsuk S, Soltani A, Khayat N (2018) Stabilization of soft clay using short fibers and poly vinyl alcohol. Geotextiles and Geomembranes, 46(5):646-655.

[155] Mirzababaei M, Miraftab M, Mohamed M, McMahon P (2013) Unconfined compression strength of reinforced clays with carpet waste fibers. Journal of Geotechnical and Geoenvironmental Engineering, 139(3):483-493

[156] Assadi-Langroudi A, Ghadr S, Theron E, Oderinde SA, Katsipatakis EM (2019) Lime cake as an alternative stabiliser for loose clayey loams. International Journal of Geosynthetics and Ground Engineering, 5(3):1-13

[157] Mirzababaei M (2021), Advances in soil fibre reinforcement. In First NiSE Workshop (NiSE1), 11-12 February, University of East London, London, UK.

[158] Assadi-Langroudi A (2021) On mechanics of porous granular matters. In First NiSE Workshop (NiSE1), 11-12 February, University of East London, London, UK.

[159] Pye K (1987) Eolian Dust and Dust Deposits. London, Academic Press

[160] Krinsley DH, Doornkamp JC (1973) Atlas of Quartz Sand Surface Textures. London, Syndics of the Cambridge University Press

[161] Ghadr S, Assadi-Langroudi A, Hung C, O'Kelly BC, Bahadori H, Ghodsi T (2020) Stabilization of sand with colloidal nano-silica hydrosols. Applied Sciences, 10(15):5192. https://doi.org/10.3390/app10155192

[162] Ghadr S, Assadi-Langroudi A, Hung C (2020) Stabilisation of peat with colloidal nanosilica. Mires and Peat: 26(Art 9)

[163] Kua TA, Arulrajah A, Mohammadinia A, Horpibulsuk S, Mirzababaei M (2017) Stiffness and deformation properties of spent coffee grounds based geopolymers. Construction and Building Materials, 138:79-87.

[164] Arulrajah A, Yaghoubi M, Disfani MM, Horpibulsuk S, Bo MW, Leong M (2018) Evaluation of fly ash-and slag-based geopolymers for the improvement of a soft marine clay by deep soil mixing. Soils and Foundations, 58(6):1358-1370

[165] Horpibulsuk S, Phetchuay C, Chinkulkijniwat A (2012) Soil stabilization by calcium carbide residue and fly ash. Journal of Materials in Civil Engineering, 24(2):184-193

[166] Hoy M, Horpibulsuk S, Arulrajah A (2016) Strength development of recycled asphalt pavement–fly ash geopolymer as a road construction material. Construction and Building Materials, 117:209-219

[167] Shekhawat P, Sharma G, Singh RM (2020) Potential application of heat cured eggshell powder and fyash-based geopolymer in pavement construction. International Journal of Geosynthetics and Ground Engineering, 6(2):1-17.

[168] Dade-Robertson M, Mitrani H, Rodriguez-Corral J, Zhang M, Hernan L, Guyet A, Wipat A (2018) Design and modelling of an engineered bacteria-based pressure-sensitive soil. Bioinspiration and Biomimetics 13(4):046004

[169] Rodriguez Corral J, Mitrani H, Dade-Robertson M, Zhang M, Maiello P (2020) Agarose gel as a soil analogue for development of advanced bio-mediated soil improvement methods. Canadian Geotechnical Journal, 57(12):2010-2019

[170] Dade-Robertson M, Corral JR, Mitrani H, Zhang M, Wipat A, Ramírez-Figueroa C, Hernan L (2016) Thinking Soils: a synthetic biology approach to material-based design computation ACADIA

[171] Hodaei M, Maghoul P, Popplewell N (2020) An overview of the acoustic studies of bone-like porous materials, and the effect of transverse acoustic waves. International Journal of Engineering Science, 147: 103189

[172] Liu H, Maghoul P, Shalaby A (2020) Laboratory-scale characterization of saturated soil samples through ultrasonic techniques. Nature Scientific Reports, 10, 3216.

[173] Liu H, Maghoul P, Shalaby A (2021) A poro-elastodynamic forward solver for dispersion analysis of saturated multilayer systems. In Barla M, Di Donna A, Sterpi D (Eds). Challenges and Innovations in Geomechanics. IACMAG 2021. Lecture Notes in Civil Engineering. 126:637-644

[174] Tagarelli V, Cotecchia F (2020) Deep Movements in Clayey Slopes Relating to Climate: Modeling for Early Warning System Design. Research for Land Protection and Development. CNRIG 2019. Lect. Notes Civil Eng. 40.

[175] Tagarelli V, Cotecchia F. (2020) The Effects of Slope Initialization on the Numerical Model Predictions of the Slope-Vegetation-Atmosphere Interaction. Geosciences, 10:85.

List of Figures

Fig. 1 (a) NiSE five principal aims and interlinked deliverables; (b) NiSE deliverables as indicators of materials' performance, measured by a traffic-light scoring system: the framework can be applied to candidate stabilising materials in any project

Fig. 2 Qualitative picture of aggregation during MD simulations; Clay platelets' orientations according to the φ angle (0° representing alignment of normal vector of platelets with the *z* axis) [14]

Fig. 3 Simulation of uniaxial compression of highly porous particulate matters through importing the "diffusion-limited aggregation" algorithm into 3D DEM software package PFC3D [11]

Fig. 4 Left: aluminium die casting and significance of identifying areas of potential weakness [15]; Right: coupled LBM-DEM simulations and time-resolved synchrotron X-ray radiography applied to the study of complex stress–strain behaviour of globular Al–Cu alloys and links to critical-state soil mechanics [12]

Fig. 5 Examples of molecular modelling and their application in geomechanics in the context of NiSE: (a) molecular dynamics (MD) simulation of minimized and equilibrated kerogen–calcite system that is useful for calculating the non-bonded interactions between the organic matter and calcite in porous soils ([23] – with some modifications); (b) variation of shear strain (creep) with potential energy against number of loading/unloading cycles in C-S-H [26]; (c-d) crystal structure and forcefield for a complex multi-body NS–kaolinite–sulphates system [25]

Fig. 6 For threshold fines content of 30 to 40%: (a) maximum static flow potential [45]; (b) equal idealised micro- and macro-void ratios [35]; (c) changing fabric from RLP to RCP as fines content increases beyond the 30 to 40% threshold [32 – with permission from ASCE]; (d) maximum liquefaction risk [35]

Fig. 7 DEM–DFD coupled simulation for a gap-graded material showing the greater ability of fines to transmit effective stress through the pore network [36]

Fig. 8 Typical microcomputer tomography laboratory setup [14]

Fig. 9 (a) Example of a network model for simulating the migration of base particles (e.g., clay, nano-stabilising agent, biopolymer nuclei) through the network, where the size of the edge of the network is determined from CSD, informed by µCT [60]; (b) Criteria, whether a base particle would move through the constriction, whether it would be trapped, and when it would be retained in the void space [60]; (c) An example of determining CSD as a function of 15% percentile of particle size [59]

Fig. 10 Soil flow mechanism as a T-bar penetrates stiff clay and pushes through an underlying soft clay stratum – D_t is the bar diameter; *d* is its vertical displacement and *x* is its horizontal displacement [67].

Fig. 11 Interior of the X-ray chamber accommodating miniature triaxial cell [70]

Fig. 12 Reconstructed 3D greyscale images of triaxial mini-specimen at three axial strains and three views (XY, XZ and 3D), followed by spatial distribution of fibres and 3D distribution of fibre orientation and length at three axial strains (reproduced from [70])

Fig. 13 (a) BIONICS research embankment, in northern England, covered to the north with grasses (e.g., *Alopecurus pratense* and *Lolium perenne*) and to the south with wildflowers (e.g., *Leucanthemum vulgare*, *Filipendula ulmaria*, *Achillea millefolium* and *Knautia arvensis*). Instrumentations allow measurement of volumetric water content, electrical conductivity and soil temperature [73]; (b) Pisciolo hillslope in southern Italy covered with (c) C3-cycle *leguminous* and (d) C4-cycle *Gramineae* plants [87]

Fig. 14 Signatures of natural biocementation in sandstone: (a) Bryce Canyon National Park, Utah, USA [89]; (b) Arches National Park, Utah, USA [90]; (c) The Belogradchik, Vidin, Bulgaria [91]

Fig. 15 (a): Bacterial life cycle and biofilm formation [94]; (b): possible forms of bacterial growth on soil particle surface [104 – with permission from ASCE]; (c): clean Ottawa sand ($D_{50} = 120\ \mu m$) packed to a void ratio of 0.6 (left), transformed into Dextran-mediated sand (middle), where particles are coated and bridged at the cost of a decrease in porosity, and hence permeability [96]

Fig. 16 MICP trials in three scales: (a) cubic meter sand box [102] – photograph from [116]; (b) 100 cubic meter sand box [108]; (c) 1000 cubic meter field-scale mediation [102]; (d) MICP at large scale: MICP-treated 400-mm dia. column by Soletanche-Bachy [117]

Fig. 17 3D visualization of the X-ray CT data illustrating the variation in porosity: (a) pre-MICP precipitation; (b) post-MICP precipitation; (c-d) service time under acidic conditions in favour of $CaCO_3$ dissolution [109]

Fig. 18 EICP trials at field-scale: soil column in box test set-up with TAM and packer, and needle penetrometer measurements done on cemented soil section [122 – with permission from ASCE]

Fig. 19 (a-b) MID test setup in Portland, Oregon, USA: injection probe and monitoring installation, including cross-hole and downhole TREX sensor array measuring excess porewater pressure, V_p and V_s, and CTD divers; (c) measuring fluid volume and salinity, and TEROS-12 sensors; (d) measuring salinity and temperature; (e) P- and S-wave velocity cross-hole measurements [128]

Fig. 20 Comparison between MICP and BPST processes [123]. Note, in Fig. 20c rods represent soil particles and red-coloured lines represent biopolymer chains, with adhesive force among themselves and cohesive force between them and the soil particles

Fig. 21 Influence of fungal mycelial networks on soil behaviour: (a) growth of *Pleurotus ostreatus* edible fungi in soil; (b-c) growth of fungi in a column of sand; (d) water repellency [139]

Fig. 22 Consolidated-undrained (CU) behaviour of sands and fibre-reinforced sands under cyclic and anisotropic loading conditions (a and b): first and second stress–strain hysteresis loops for two sands, mixed with silt and fibre [35]; (c): HCTS CU results for sand, with and without fibre reinforcement, showing stress–strain curves for p' = 400 kPa, α = 30°, and b = 0.5 and 1.0 (compression and torsion) [68]; (d) HCTS results for sand, with and without fibre reinforcement showing stress–strain curves for p' = 400 kPa, α = 60°, b = 0.5 and 1.0 (torsion). Note: HCTS, hollow cylinder torsional shear; p', effective mean normal stress; α, principal stress orientation to vertical direction; b, intermediate principal stress ratio [68]

Fig. 23 Examples of natural, synthetic and recycled fibres sometimes mixed in soil to imitate plant rootlet reinforcement effect: (a) coir [157]; (b) nylon – virgin synthetic [157]; (c) polypropylene – virgin synthetic [157]; (d) fibreglass – virgin synthetic [157]; (e-f) waste carpet [155]; (g) jute [153 – with permission from ASCE]; (h): coir [70]; (i) thermoplastic polymeric microsynthetic [68]; (j) granulated tyre [158]

Fig. 24 Sculpting soil responses to force by altering sequences of DNA and through the interaction of many different genetic devices and engineered organisms: (a) artists impression of a bio-based self-constructing foundation [169]; (b) unconfined compression performed on a column of agarose gel [170]; (c) microstructure of Agarose LM gel [169]; (d) simulation of multilateral flow (growth media for bacteria) and implications of 3D architecture of cementation in sands [119]; (e-f) 3D sand forms, scanned as excavation takes place, in seeking an insight into cementation process [119]

Figure 1

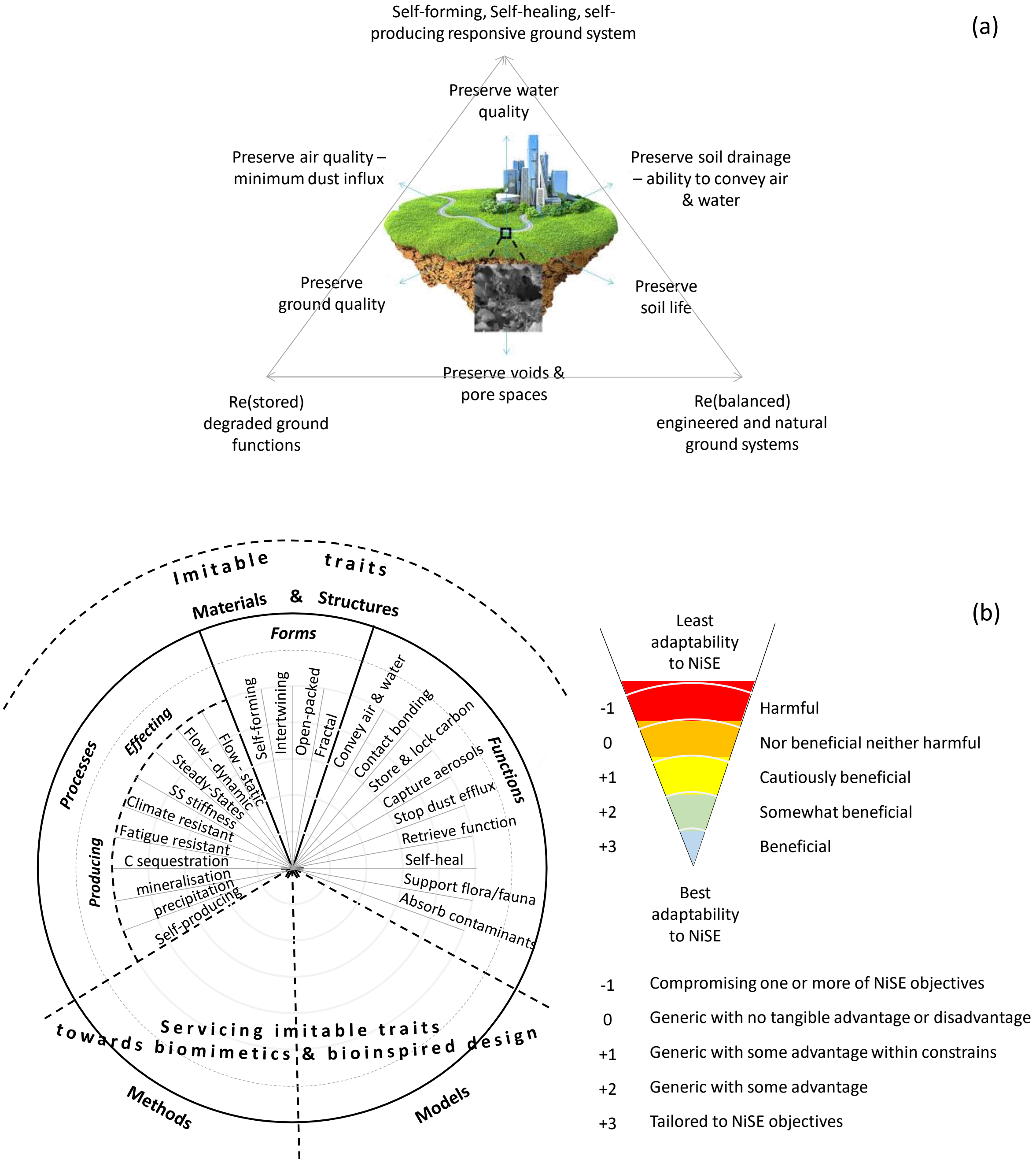
(a)
Self-forming, Self-healing, self-producing responsive ground system
Preserve water quality
Preserve air quality – minimum dust influx
Preserve soil drainage – ability to convey air & water
Preserve ground quality
Preserve soil life
Preserve voids & pore spaces
Re(stored) degraded ground functions
Re(balanced) engineered and natural ground systems
(b)
Imitable traits
Materials & Structures
Forms
Self-forming
Intertwining
Open-packed
Fractal
Convey air & water
Contact bonding
Store & lock carbon
Capture aerosols
Stop dust efflux
Retrieve function
Self-heal
Support flora/fauna
Absorb contaminants
Functions
Processes
Effecting
Flow - static
Flow - dynamic
Steady-States
SS stiffness
Climate resistant
Fatigue resistant
Producing
C sequestration
mineralisation
precipitation
Self-producing
Servicing imitable traits
towards biomimetics & bioinspired design
Methods
Models
Least adaptability to NiSE
-1
Harmful
0
Nor beneficial neither harmful
+1
Cautiously beneficial
+2
Somewhat beneficial
+3
Beneficial
Best adaptability to NiSE
-1 Compromising one or more of NiSE objectives
0 Generic with no tangible advantage or disadvantage
+1 Generic with some advantage within constrains
+2 Generic with some advantage
+3 Tailored to NiSE objectives

Figure 2

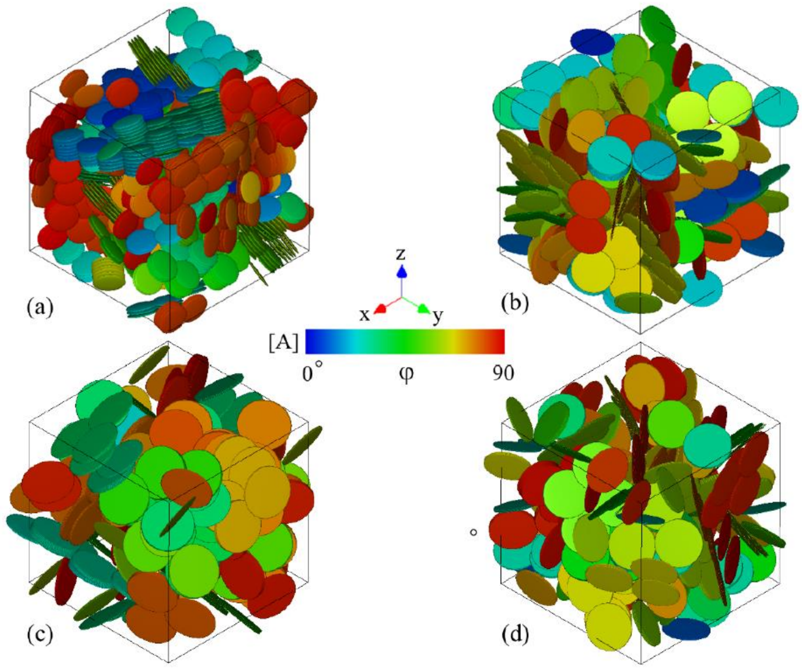

Figure 3

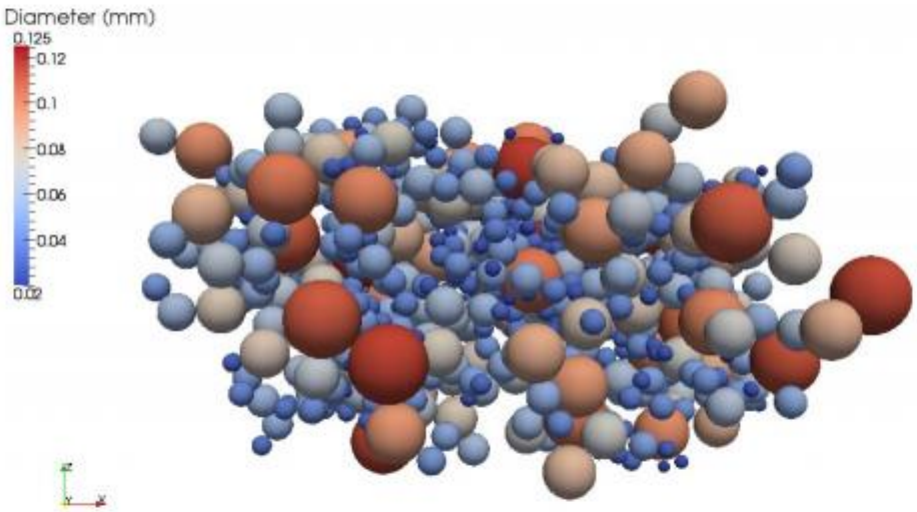

Figure 4

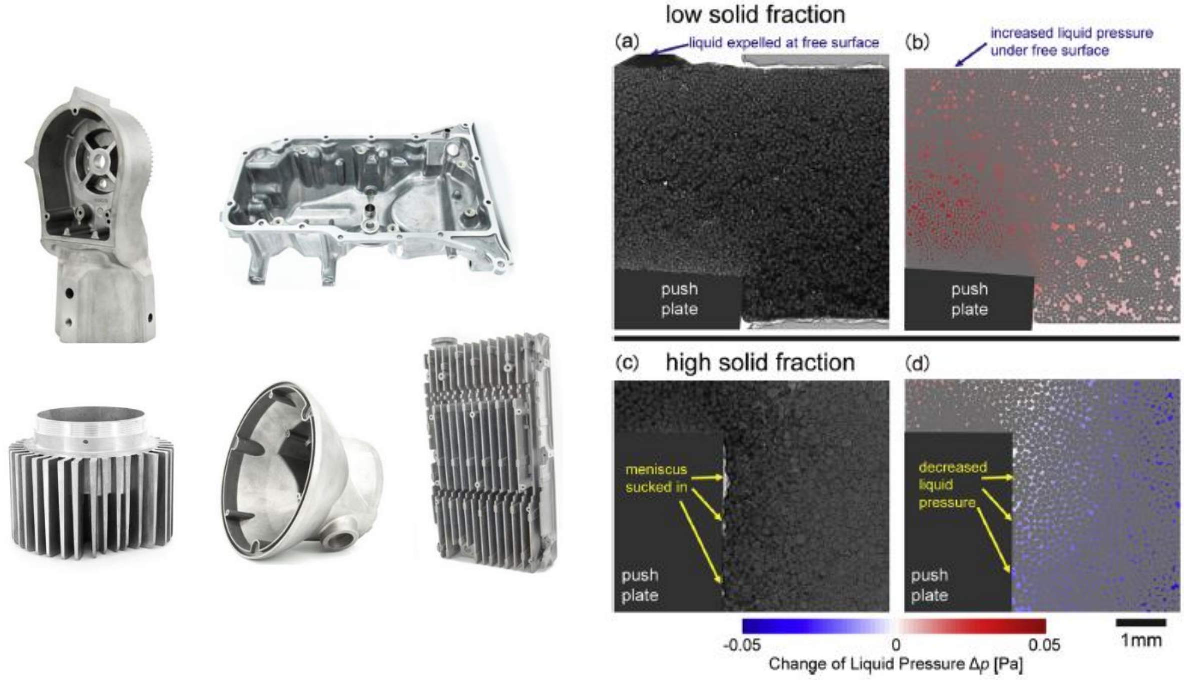

low solid fraction
(a)
liquid expelled at free surface
(b)
increased liquid pressure under free surface
push plate
push plate
(c)
high solid fraction
(d)
meniscus sucked in
push plate
decreased liquid pressure
push plate
-0.05
0
0.05
1mm
Change of Liquid Pressure Δp [Pa]

Figure 5

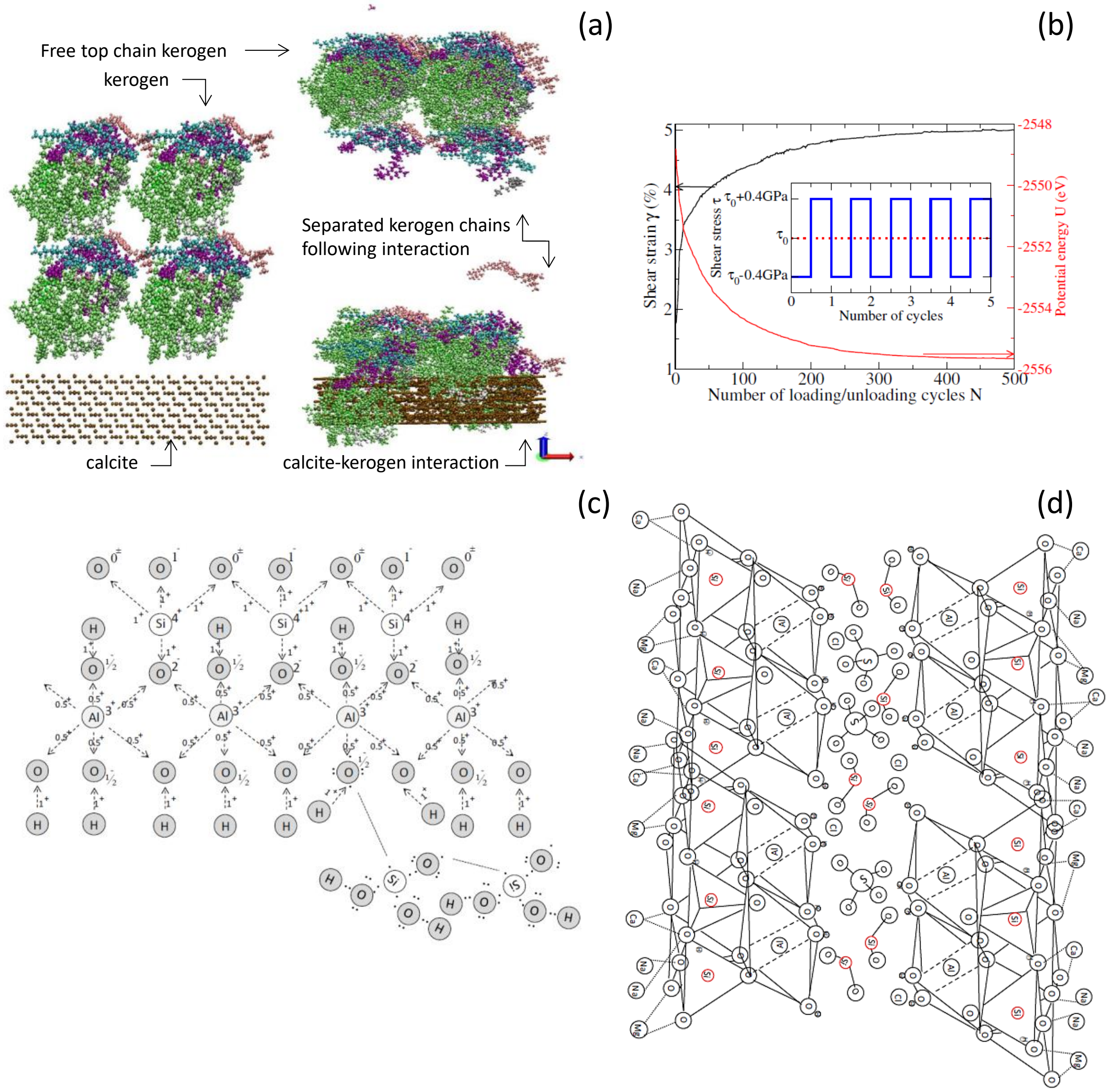
(a)
(b)
(c)
(d)
Free top chain kerogen
kerogen
Separated kerogen chains following interaction
calcite
calcite-kerogen interaction
Shear strain γ (%)
Potential energy U (eV)
Number of loading/unloading cycles N
Shear stress τ
τ0+0.4GPa
τ0
τ0-0.4GPa
Number of cycles

Figure 6

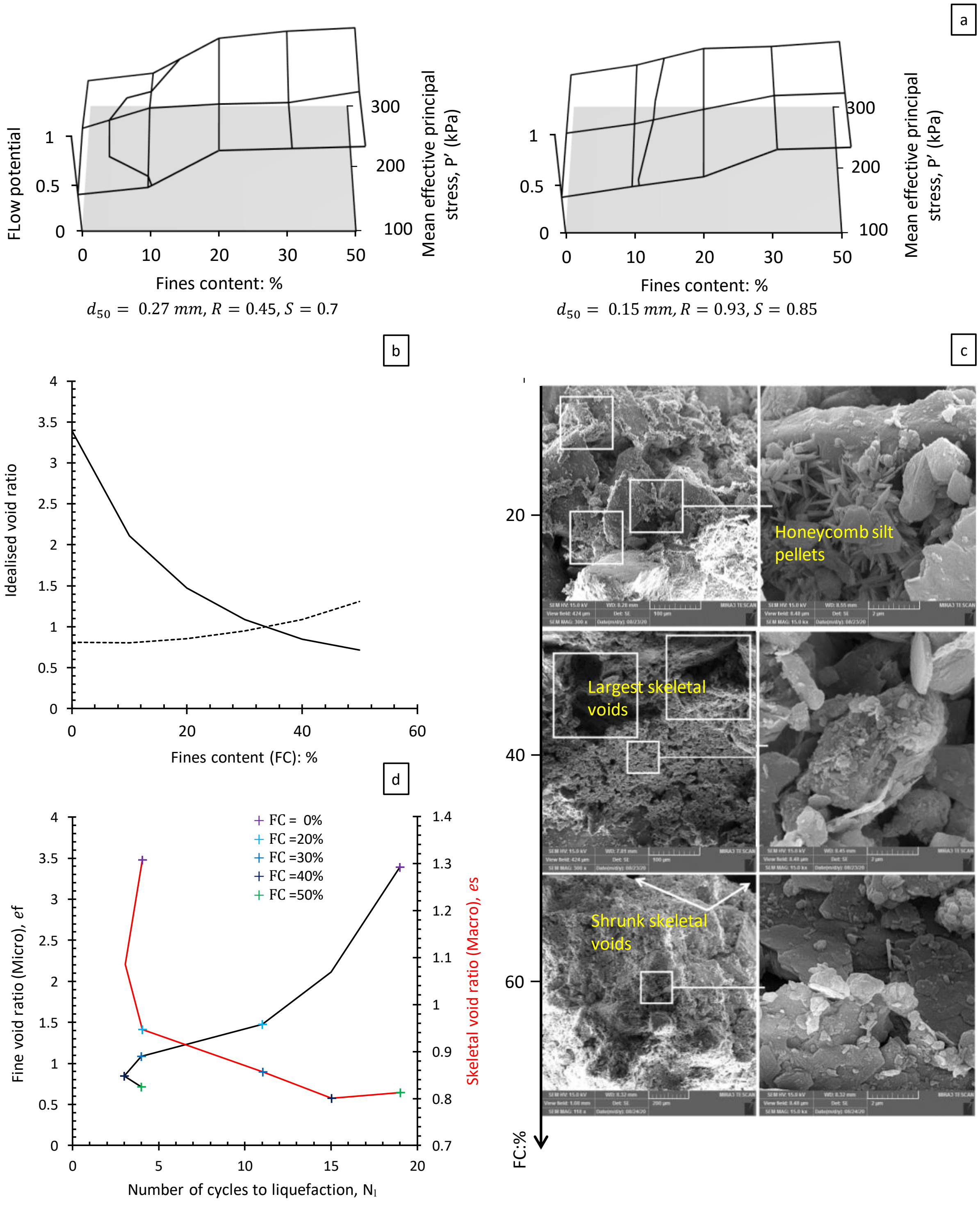
a
FLow potential
1
0.5
0
0
10
20
30
50
300
200
100
Mean effective principal stress, P' (kPa)
Fines content: %
$d_{50} = 0.27\ mm, R = 0.45, S = 0.7$
$d_{50} = 0.15\ mm, R = 0.93, S = 0.85$
b
Idealised void ratio
4
3.5
3
2.5
2
1.5
1
0.5
0
0
20
40
60
Fines content (FC): %
c
20
40
60
FC:%
Honeycomb silt pellets
Largest skeletal voids
Shrunk skeletal voids
d
Fine void ratio (Micro), ef
Skeletal void ratio (Macro), es
FC = 0%
FC =20%
FC =30%
FC =40%
FC =50%
1.4
1.3
1.2
1.1
1
0.9
0.8
0.7
0
5
10
15
20
Number of cycles to liquefaction, Nl

Figure 7

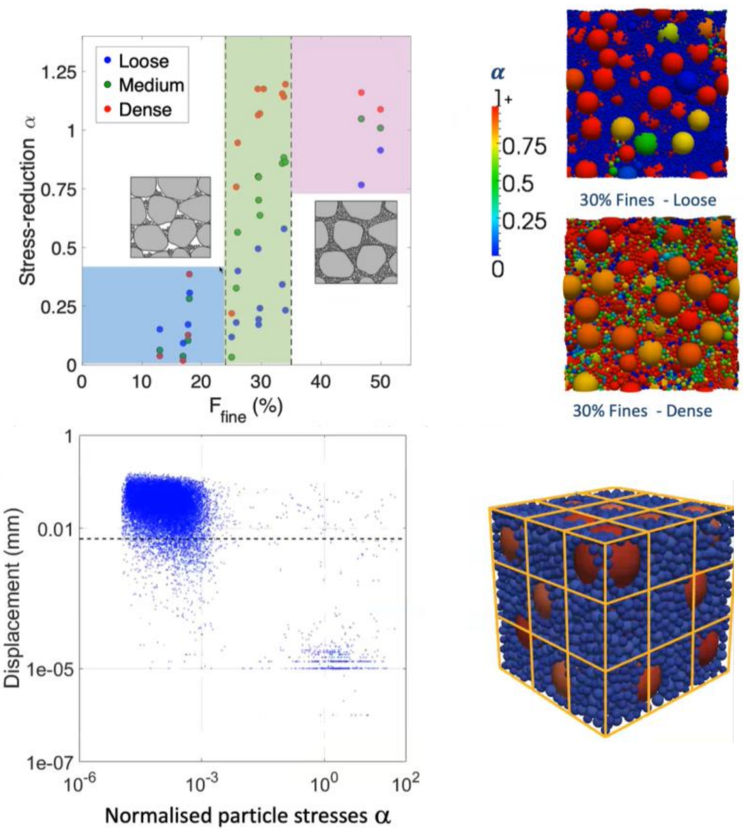

Loose
Medium
Dense
Stress-reduction α
F_fine (%)
α
30% Fines - Loose
30% Fines - Dense
Displacement (mm)
Normalised particle stresses α

Figure 8

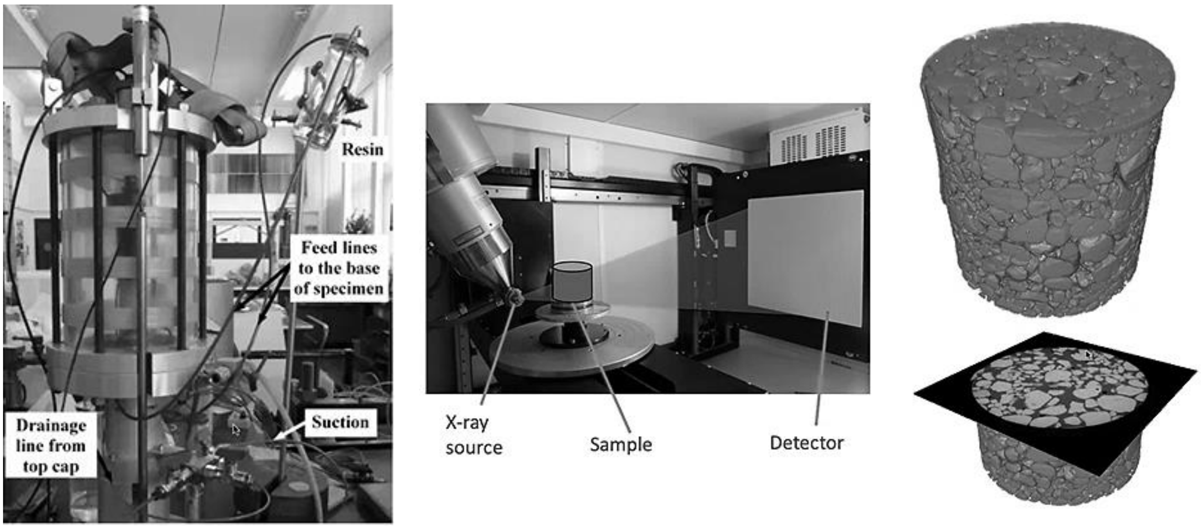
Resin
Feed lines to the base of specimen
Drainage line from top cap
Suction
X-ray source
Sample
Detector

Figure 9

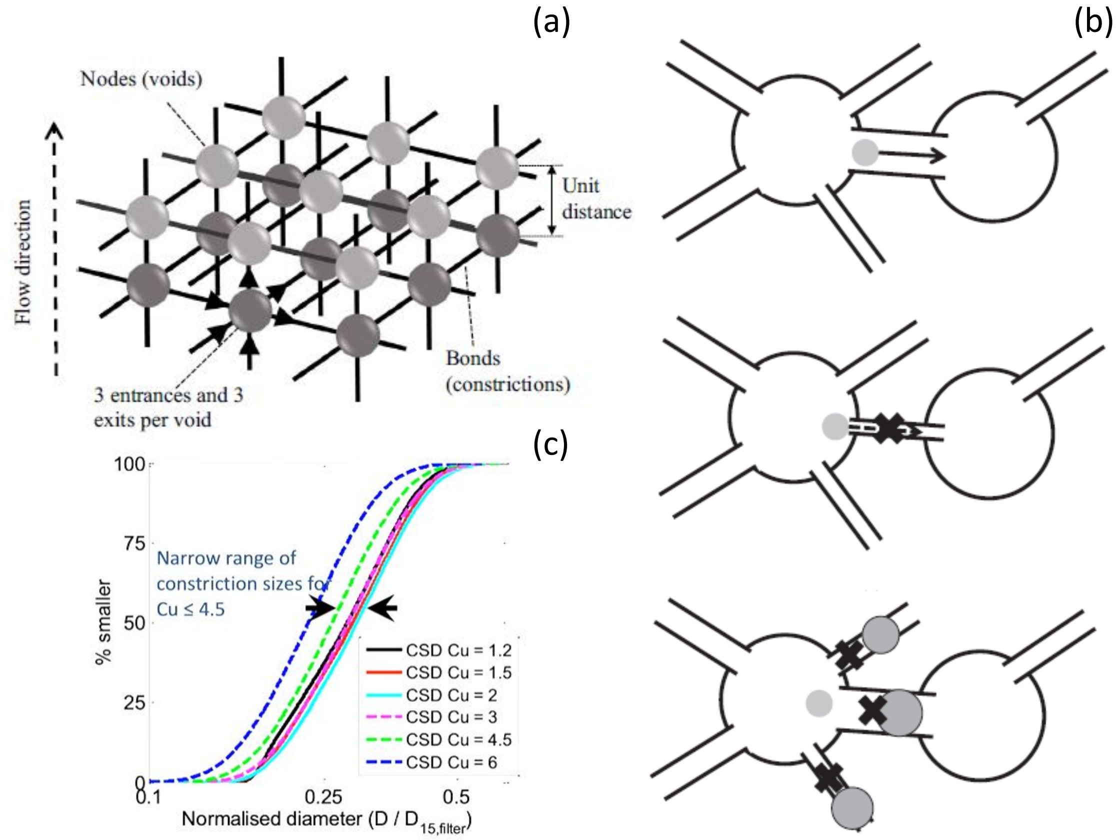
(a)
(b)
(c)
Nodes (voids)
Flow direction
Unit distance
Bonds (constrictions)
3 entrances and 3 exits per void
100
75
50
25
0
% smaller
Narrow range of constriction sizes for Cu ≤ 4.5
CSD Cu = 1.2
CSD Cu = 1.5
CSD Cu = 2
CSD Cu = 3
CSD Cu = 4.5
CSD Cu = 6
0.1
0.25
0.5
Normalised diameter (D / D15,filter)

Figure 10

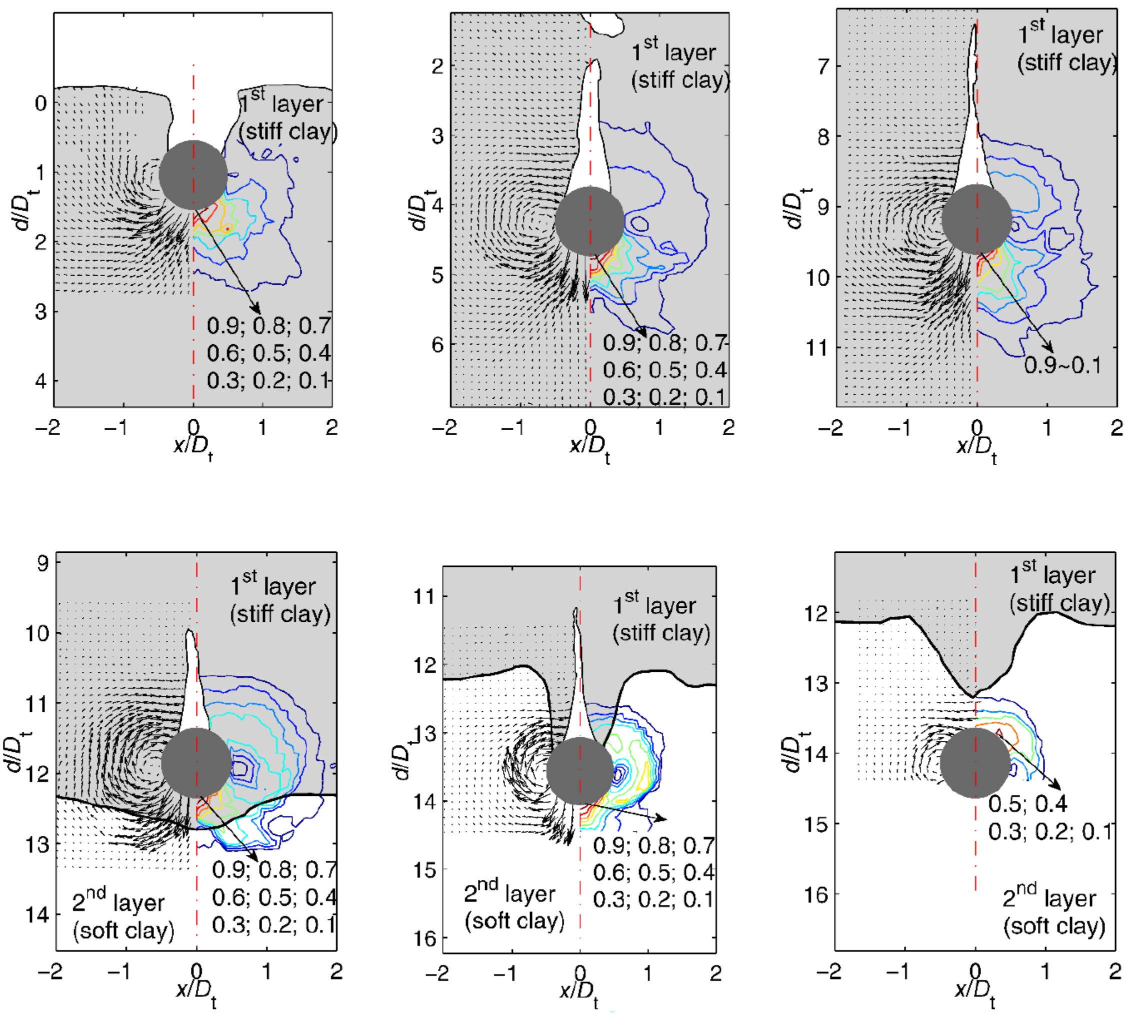

1st layer
(stiff clay)
2nd layer
(soft clay)
0.9; 0.8; 0.7
0.6; 0.5; 0.4
0.3; 0.2; 0.1
0.9~0.1
0.5; 0.4
0.3; 0.2; 0.1
d/Dt
x/Dt

Figure 11

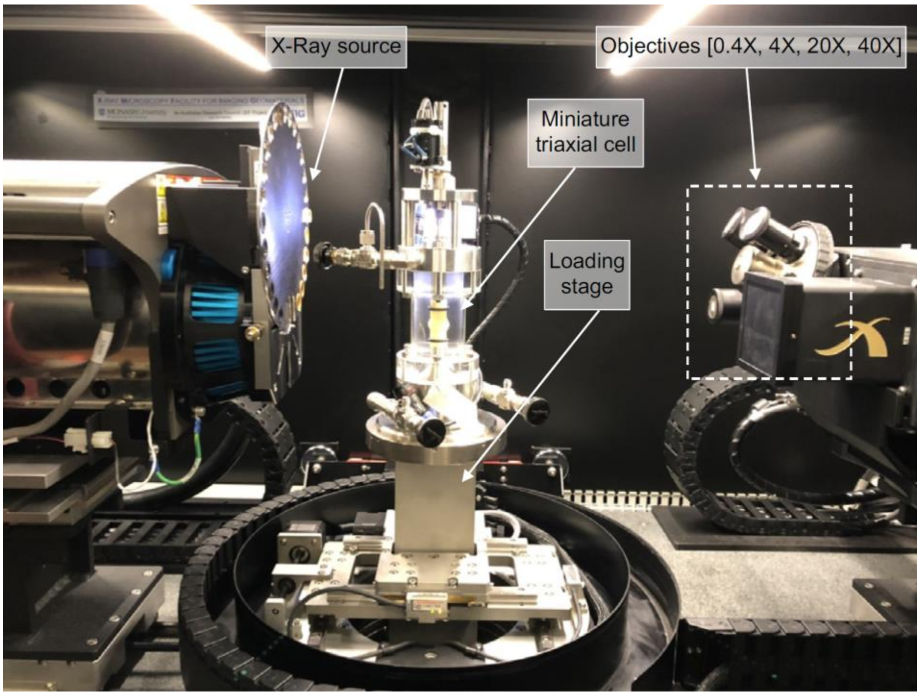
X-Ray source
Objectives [0.4X, 4X, 20X, 40X]
Miniature triaxial cell
Loading stage

Figure 12

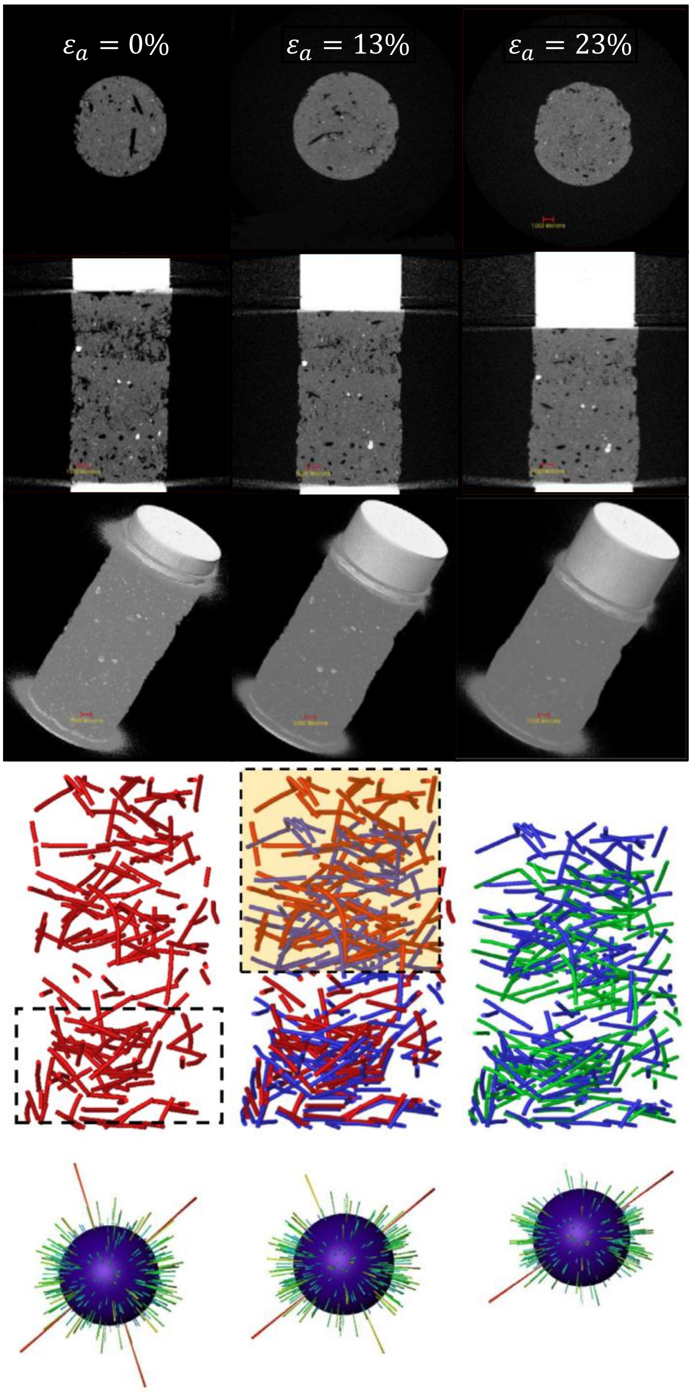

Figure 13

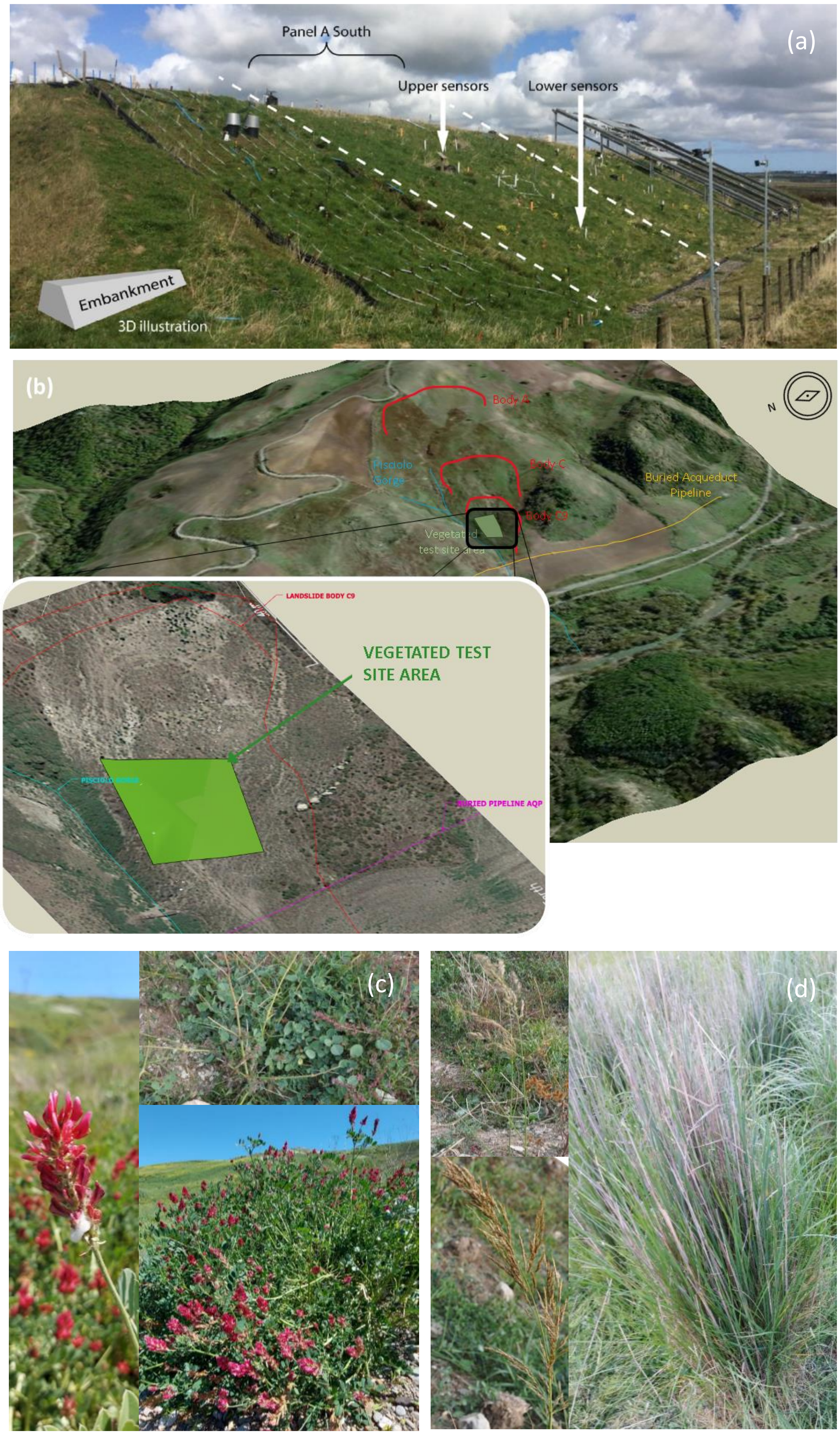
Panel A South
Upper sensors
Lower sensors
(a)
Embankment
3D illustration
(b)
Body A
Body C
Buried Aqueduct Pipeline
N
LANDSLIDE BODY C9
VEGETATED TEST SITE AREA
BURIED PIPELINE AQP
(c)
(d)

Figure 14

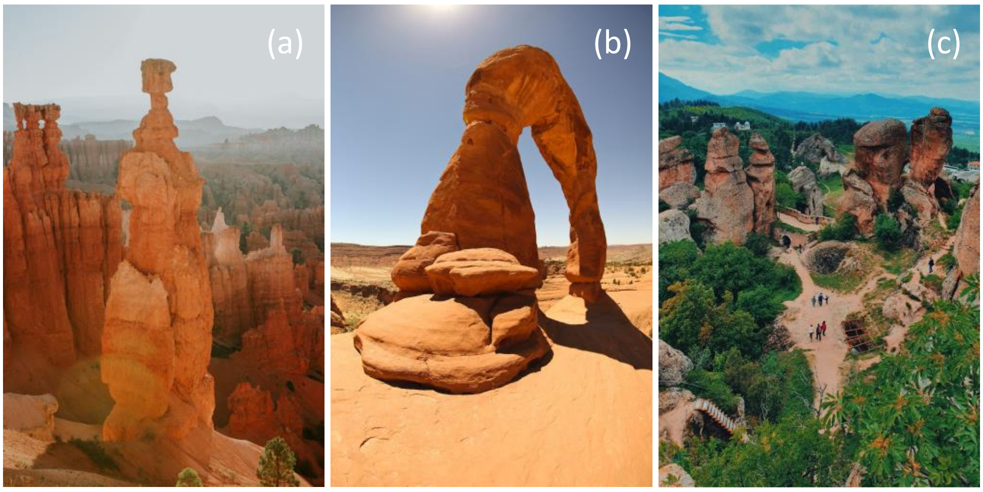

Figure 15

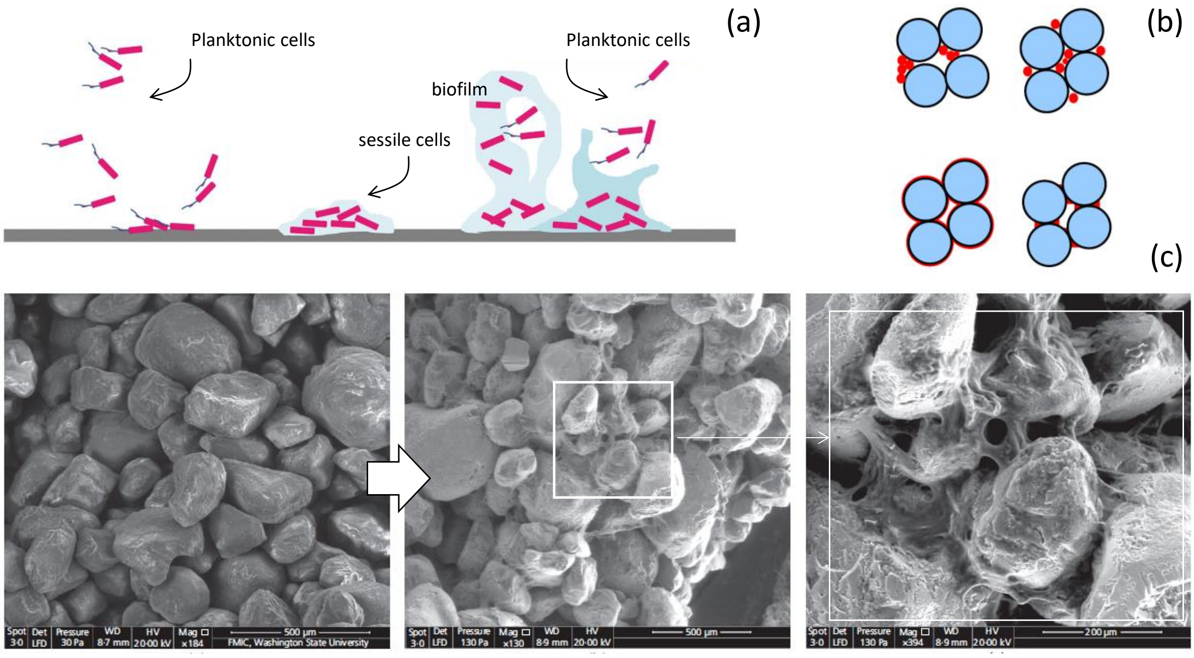
(a)
Planktonic cells
Planktonic cells
biofilm
sessile cells
(b)
(c)
500 μm
FMIC, Washington State University
500 μm
200 μm

Figure 16

Figure 17

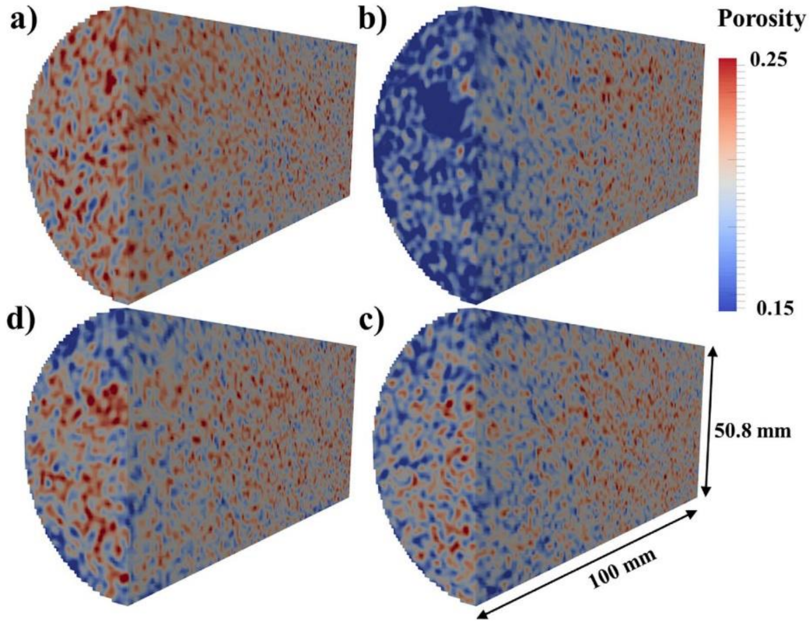

Figure 18

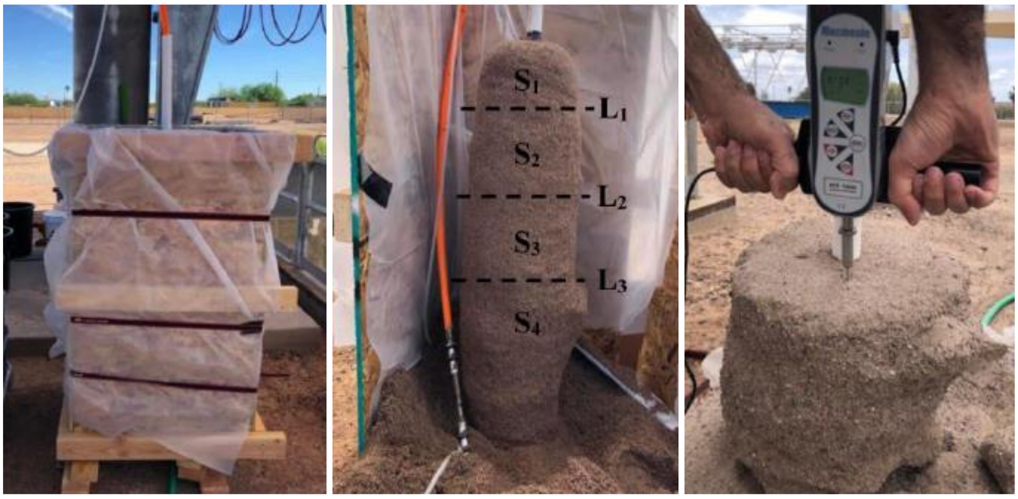

Figure 19

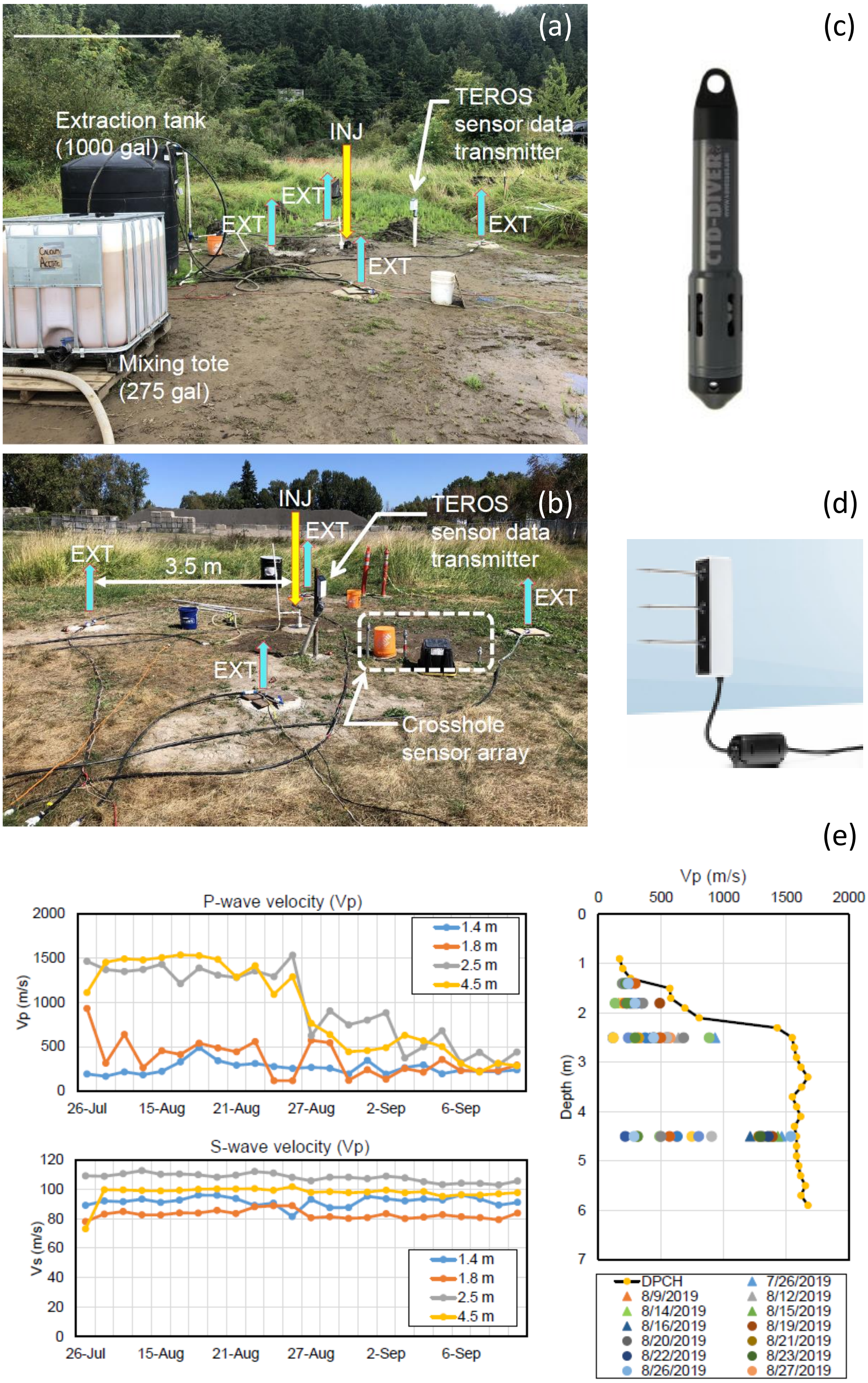

(a)
Extraction tank
(1000 gal)
INJ
EXT
TEROS
sensor data
transmitter
Mixing tote
(275 gal)
(b)
3.5 m
Crosshole
sensor array
(c)
CTD-DIVER
(d)
(e)
P-wave velocity (Vp)
Vp (m/s)
1.4 m
1.8 m
2.5 m
4.5 m
26-Jul
15-Aug
21-Aug
27-Aug
2-Sep
6-Sep
S-wave velocity (Vp)
Vs (m/s)
Vp (m/s)
Depth (m)
DPCH
7/26/2019
8/9/2019
8/12/2019
8/14/2019
8/15/2019
8/16/2019
8/19/2019
8/20/2019
8/21/2019
8/22/2019
8/23/2019
8/26/2019
8/27/2019

Figure 20

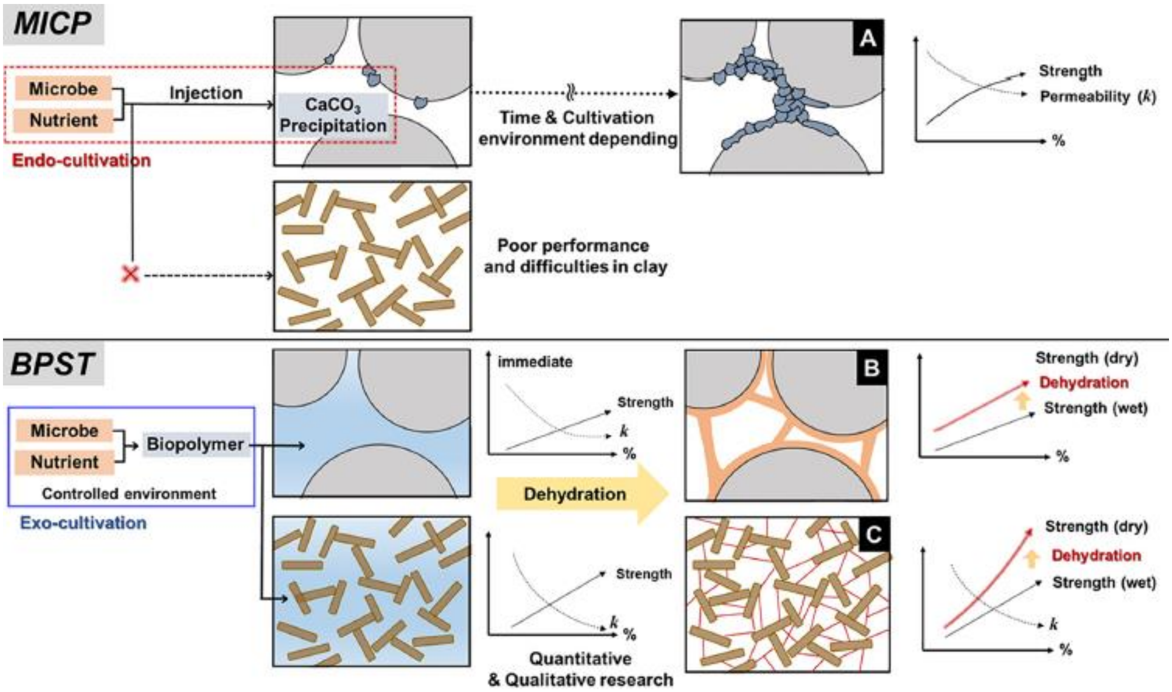
MICP
Microbe
Nutrient
Injection
CaCO3 Precipitation
Endo-cultivation
Time & Cultivation environment depending
A
Strength
Permeability (k)
%
Poor performance and difficulties in clay
BPST
Microbe
Nutrient
Biopolymer
Controlled environment
Exo-cultivation
immediate
Strength
k
%
Dehydration
B
Strength (dry)
Dehydration
Strength (wet)
%
Strength
k
%
Quantitative & Qualitative research
C
Strength (dry)
Dehydration
Strength (wet)
k
%

Figure 21

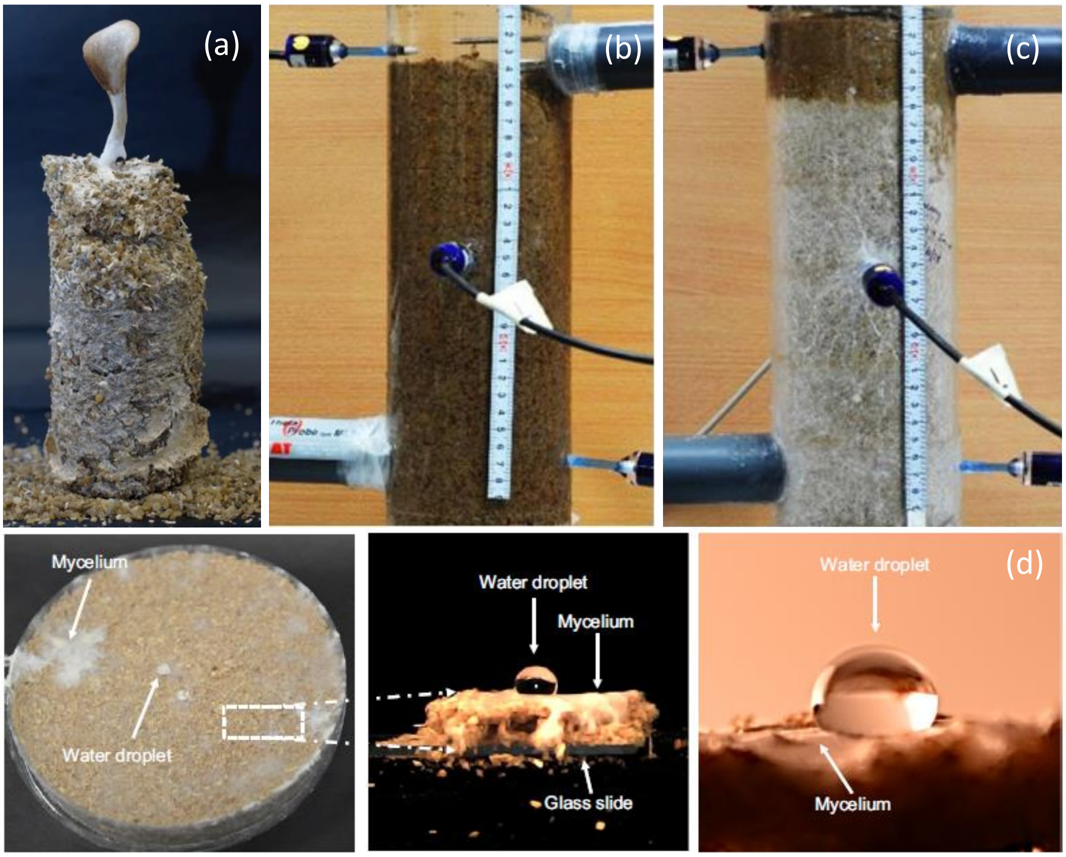

(a)
(b)
(c)
Mycelium
Water droplet
Water droplet
Mycelium
Glass slide
(d)
Water droplet
Mycelium

Figure 22

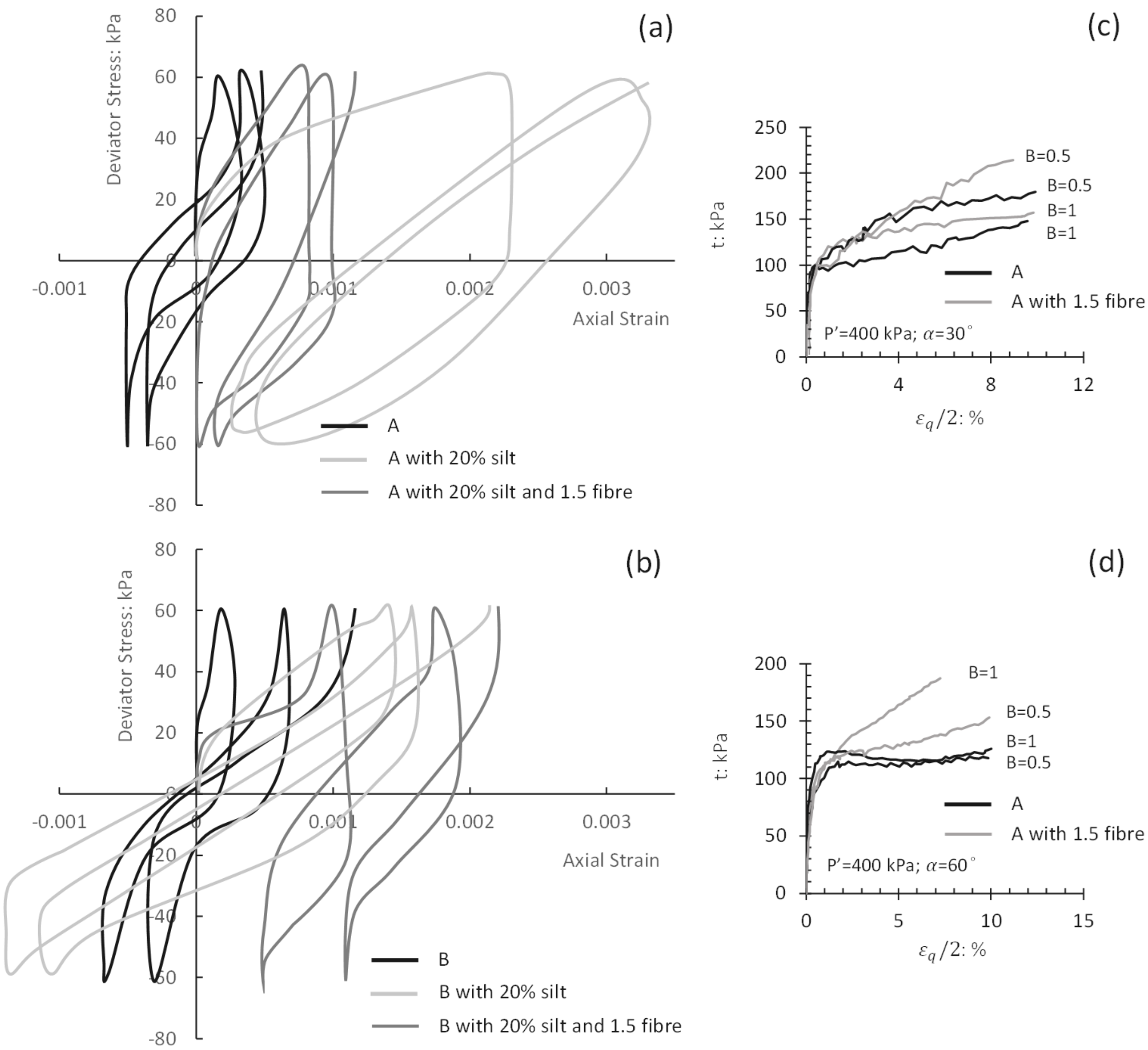
(a)
Deviator Stress: kPa
Axial Strain
A
A with 20% silt
A with 20% silt and 1.5 fibre
(b)
Deviator Stress: kPa
Axial Strain
B
B with 20% silt
B with 20% silt and 1.5 fibre
(c)
t: kPa
B=0.5
B=0.5
B=1
B=1
A
A with 1.5 fibre
P'=400 kPa; α=30°
$\varepsilon_q/2$: %
(d)
t: kPa
B=1
B=0.5
B=1
B=0.5
A
A with 1.5 fibre
P'=400 kPa; α=60°
$\varepsilon_q/2$: %

Figure 23

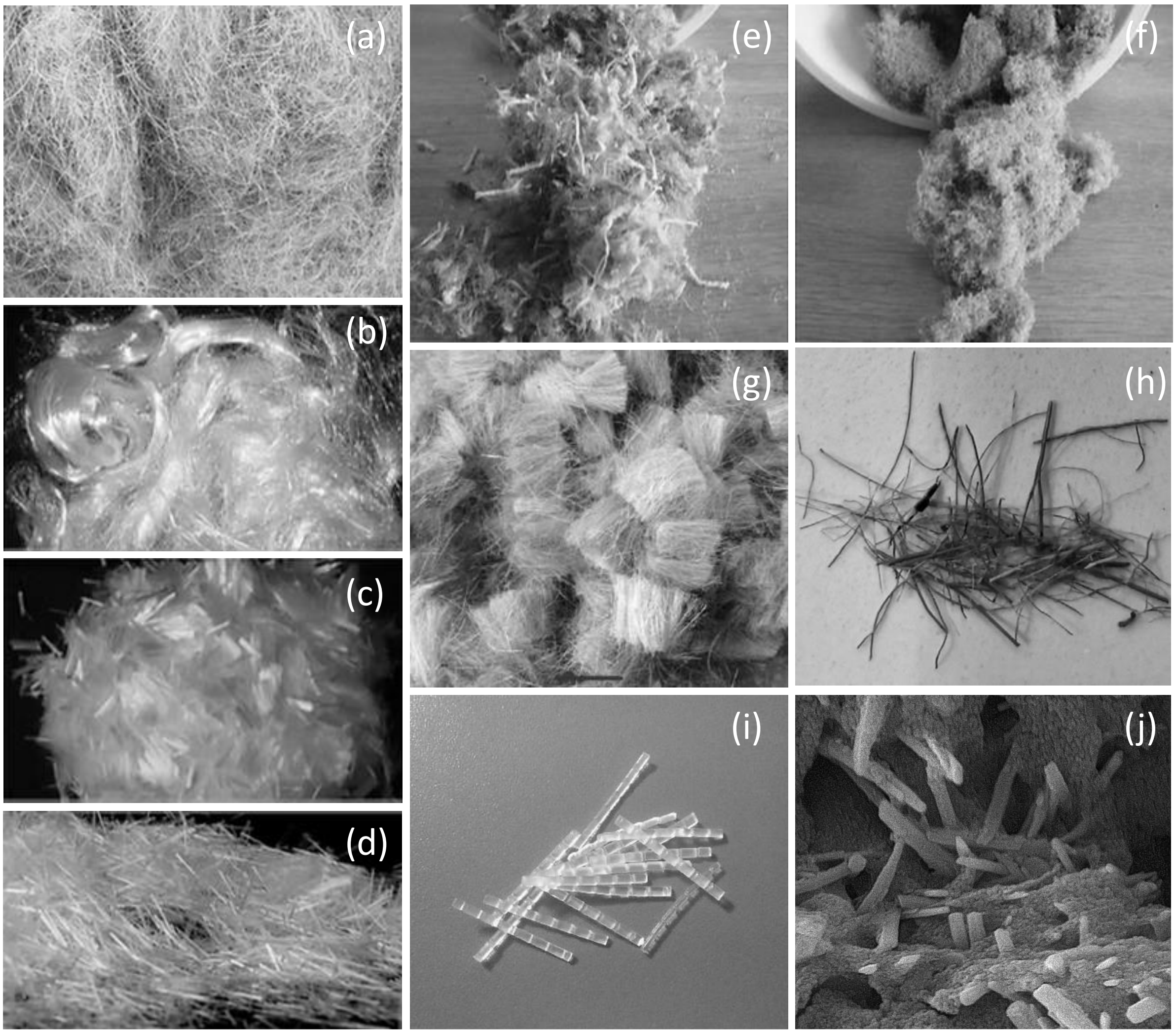

Figure 24

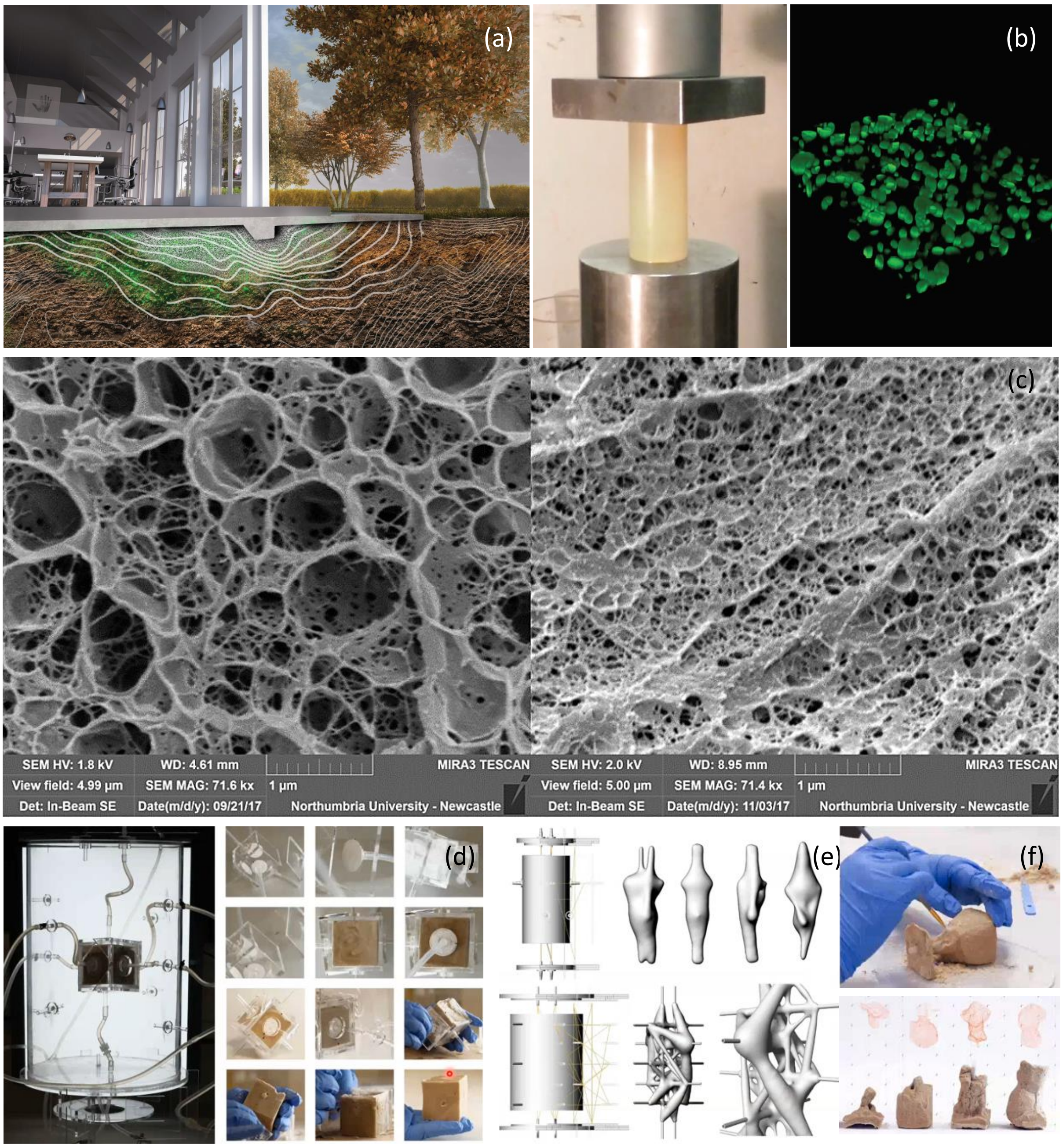
(a)
(b)
(c)
SEM HV: 1.8 kV
WD: 4.61 mm
MIRA3 TESCAN
View field: 4.99 µm
SEM MAG: 71.6 kx
1 µm
Det: In-Beam SE
Date(m/d/y): 09/21/17
Northumbria University - Newcastle
SEM HV: 2.0 kV
WD: 8.95 mm
MIRA3 TESCAN
View field: 5.00 µm
SEM MAG: 71.4 kx
1 µm
Det: In-Beam SE
Date(m/d/y): 11/03/17
Northumbria University - Newcastle
(d)
(e)
(f)